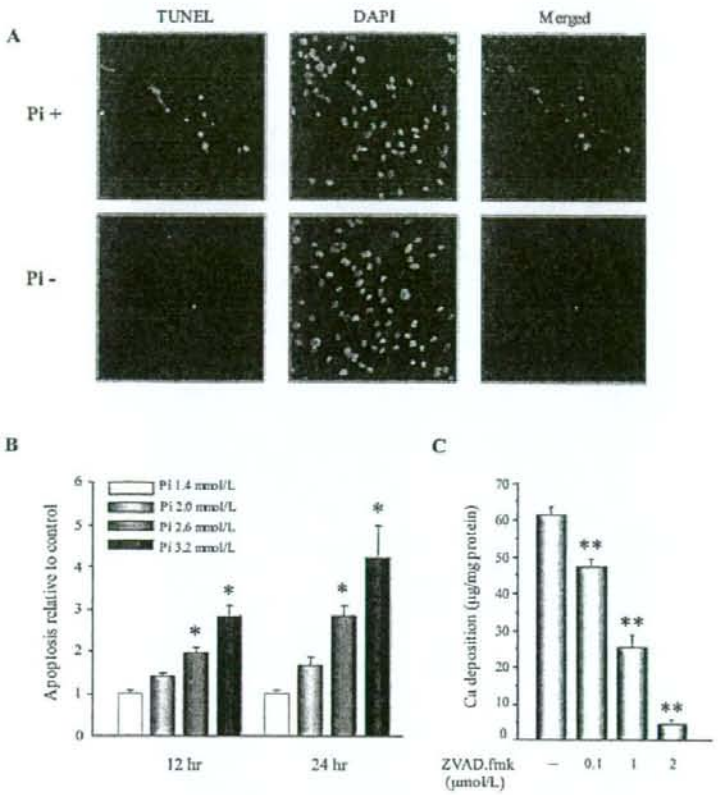

Figure 2. Pi induces apoptosis, and ZVAD.fmk inhibits Pi-induced calcification. A, After incubation with 1.4 (Pi-) and 3.2 mmol/L (Pi+) Pi for 10 days, apoptotic cells were identified by TUNEL staining (green). Nuclei were counterstained with 4',6-diamidino-2-phenylindole (DAPI) (blue). B, Serum-starved HASMC were cultured with the indicated concentration of Pi for 24 hours. A quantitative index of apoptosis, determined by ELISA, is presented as the relative value to that with 1.4 mmol/L Pi. All values are presented as mean±SEM (n=3). *$P<0.05$ vs 1.4 mmol/L Pi by Fisher's test. C, HASMC were incubated with the indicated concentration of ZVAD.fmk in the presence of 2.6 mmol/L Pi for 6 days. Ca content was measured and normalized by cell protein content. All values are presented as mean±SEM (n=6). **$P<0.01$ vs 2.6 mmol/L Pi, ZVAD.fmk(-) by Fisher's test. Experiments were performed with at least 3 different cell populations.

of the 18S RNA at each time point, and the half-life was calculated by linear extrapolation.

Preparation of Small Interfering RNA Targeting Gas6 and Transfection

Two small interfering RNAs (siRNAs) were designed to target human Gas6 (accession no. NM_000820) using siRNA design software (Dharmacon). The sequences for Gas6 were 5'-GGACCTGCCAAGACATAGA-3' and 5'-ACCTCGTGCAGCCT-ATAAA-3'. Nonspecific control siRNA was synthesized using standard templates (Dharmacon). Twenty-four hours after HASMC seeding onto 12-well plates, cells were cultured in serum-free medium for an additional 24 hours, then transfected with Gas6 (100 nmol/L) and control siRNA using transfection reagent (Upstate). To evaluate the effect of Gas6 siRNA on Ca deposition, siRNA was transfected when HASMC had reached 80% to 90% confluence and then transfected every time the medium was changed (every 2 days) up to 6 days. The loss of Gas6 by transfection of siRNA was validated by immunoblotting for Gas6 protein in the cell lysates 48 hours and 6 days after siRNA transfection.

Statistical Analysis

All results are presented as mean±SEM. Statistical comparisons were made by ANOVA, unless otherwise stated. A value of $P<0.05$ was considered to be significant.

An expanded Materials and Methods section can be found in the online data supplement available at http://circres.ahajournals.org.

Results

Statins Inhibit Pi-Induced HASMC Calcification

To induce HASMC calcification, cells were incubated with calcification medium for 10 days. We confirmed that high phosphate (≥2.6 mmol/L) induced Ca deposition in a concentration- and time-dependent manner, whereas 1.4 mmol/L Pi, equivalent to the human physiological serum phosphate level, was not able to induce Ca deposition up to 10 days. To investigate the effect of statins on Pi-induced calcification, HASMC were incubated with atorvastatin in the presence of 2.6 mmol/L Pi. On day 6, Ca deposition was significantly suppressed by atorvastatin in a concentration-dependent manner (51.1±1.9% of control at 0.1 μmol/L) (Figure 1A). An inhibitory effect of the statins on Ca deposition was also found by von Kossa's staining (Figure 1B). Atorvastatin was able to be added at as high a concentration as 0.1 μmol/L without cell damage. The inhibitory effect was also observed with fluvastatin (0.001 to 0.1 μmol/L) and pravastatin (0.01 to 50 μmol/L) (data not shown). The inhibitory effect of statins was not blocked by mevalonate (100 μmol/L), farnesylpyrophosphate (1 μmol/L), or geranylgeranylpyrophosphate (1 μmol/L), suggesting that the effect is not dependent on the mevalonate pathway (Figure 1C).

Inhibitory Effect of Statins on Calcification Is Caused by Preventing Apoptosis, Not by Inhibiting Sodium-Dependent Phosphate Cotransporter Activity

Two different time courses were tested to examine the effect of Pi on HASMC apoptosis: short-term (up to 24 hours) and long-term (up to 10 days; practical time course of calcifica-

tion process). During calcification, Pi increased the rate of apoptotic cell death detected by terminal deoxyribonucleotidyl transferase-mediated dUTP-digoxigenin nick-end labeling (TUNEL) assay (Figure 2A). Furthermore, cytoplasmic histone-associated DNA fragments determined by ELISA, as a quantitative index of apoptosis, were also increased by Pi in a concentration- and time-dependent manner in both short-term (Figure 2B) and long-term conditions (supplemental Figure I). In addition, caspase 3 activation, detected by immunoblotting, by 2.6 mmol/L Pi was observed in short-term and long-term conditions (data not shown). To investigate the relationship between apoptosis and calcification, we used ZVAD.fmk, a general caspase inhibitor. We found that ZVAD.fmk significantly inhibited Pi-induced apoptosis as well as calcification in a concentration-dependent manner (Figure 2C).

It has been reported that sodium-dependent phosphate cotransporter (NPC) activity is an important pathway regulating Pi-induced HASMC calcification.[25] We confirmed that type III NPC (Pit-1) was expressed in the HASMC that we used, and its activity was enhanced by Pi treatment. Furthermore, a specific inhibitor of NPC, phosphonoformic acid (PFA), inhibited Ca deposition (reduced by 90.4% at 0.1 μmol/L), indicating that NPC-mediated Pi uptake is also essential for HASMC calcification.

To investigate the mechanisms of these statins, we examined the effect of atorvastatin on apoptosis and NPC activity. Atorvastatin, at concentrations exerting inhibition of calcification, reduced apoptosis in a concentration-dependent manner (Figure 3A). A beneficial effect of statins was also observed in the long-term condition (supplemental Figure II). On the other hand, statins did not inhibit NPC activity induced by Pi treatment (Figure 3B).

Downregulation of Gas6-Axl Interaction Is Associated With Pi-Induced Apoptosis

Immunoblot analysis showed that the expression of Gas6 and Axl was markedly downregulated by 2.6 mmol/L Pi in both short-term (Figure 4A) and long-term (supplemental Figure III) conditions. To further examine whether Pi affects the secretion of Gas6 by HASMC, conditioned medium was collected after Pi treatment. Gas6 production in the medium was reduced by 2.6 mmol/L Pi, along with a reduction in its intracellular expression (Figure 4B). Gas6 production was also reduced in an immunoprecipitation-immunoblotting study on day 10 (Figure 4C). Next, to investigate the role of Gas6-Axl interaction in the process of apoptosis and calcification, rhGas6 and Axl-ECD were supplemented in Pi-treated HASMC. The addition of rhGas6 significantly inhibited both Pi-induced apoptosis and calcification. Addition of Axl-ECD to block the binding of Gas6 to Axl clearly abrogated the inhibitory effect of rhGas6 (Figure 4D and 4E). These results indicate that Pi-induced apoptosis and calcification are associated with downregulation of the Gas6-Axl interaction.

Statin-Mediated Induction of Gas6 Expression Is Dependent on mRNA Stabilization, Not on Transcription

To investigate whether the antiapoptotic effect of statins is dependent on restoration of the Gas6-Axl interaction, we first assessed the effect of statins on Gas6 expression. As shown in Figure 5A, atorvastatin increased Gas6 expression, which was downregulated by Pi at both the mRNA and protein levels. Upregulation of Gas6 expression was also observed in the long-term condition (supplemental Figure IV). Furthermore, to elucidate the mechanism of statins on restoration of Gas6 mRNA, a promoter study was undertaken. Reporter assay using the −1.9 kb Gas6-luciferase DNA construct revealed that atorvastatin did not have a significant effect on Gas6 promoter activity (supplemental Figure V), as well as mRNA expression under the condition in which it was significantly inhibited by PDGF-BB (data not shown). Next, we investigated the effect of atorvastatin on mRNA stabilization using an RNA polymerase inhibitor, actinomycin D (ActD). As shown in Figure 5B, Gas6 mRNA expression was more stable in the presence of atorvastatin than in its absence under Pi and ActD treatment. The half-life was 15.9 hours with atorvastatin and 5 hours without atorvastatin, suggesting the capacity of statins to improve Gas6 mRNA stabilization (Figure 5C). Taken together, these findings suggest that the restoration of Gas6 mRNA by statins appears to be mediated by decreasing the mRNA degradation rate, and not by stimulating transcriptional activity.

Furthermore, to determine whether Gas6 is required for statin-mediated effects, we tried to knock down the action of

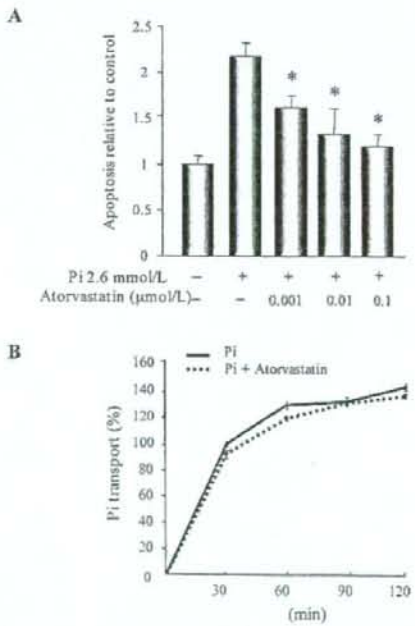

Figure 3. Effect of atorvastatin on Pi-induced apoptosis and NPC activity. A, HASMC were cultured with the indicated concentration of atorvastatin for 12 hours and then incubated with 2.6 mmol/L Pi for an additional 24 hours. All values are presented as mean±SEM (n=3). *$P<0.05$ vs 2.6 mmol/L Pi, statin (-) by Fisher's test. B, HASMC were treated with (dotted line) or without (solid line) 0.1 μmol/L atorvastatin in the presence of 2.6 mmol/L Pi. On day 6, NPC activity was determined in Earl's balanced salt solution containing 0.1 mmol/L $H_3{}^{32}PO_4$ (1 μCi/mL) with 143 mmol/L sodium chloride for the indicated period. All values are presented as mean±SEM (n=6).

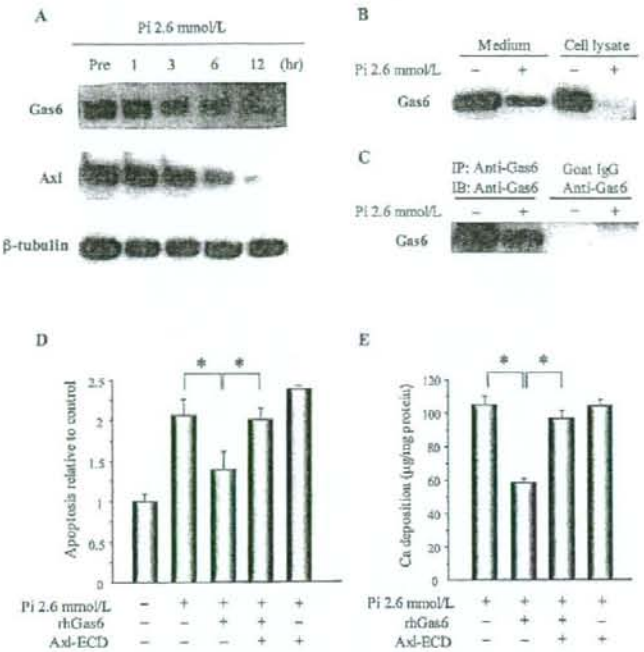

Figure 4. Pi reduces production of Gas6 and Axl, and rhGas6 inhibits Pi-induced apoptosis and calcification via Axl. A, HASMC were cultured in the presence of 2.6 mmol/L Pi for 12 hours. Cell lysates were subjected to SDS-PAGE followed by immunoblotting with antibodies to Gas6, Axl, or β-tubulin. B, Conditioned medium of HASMC in the absence (lane 1) or presence (lane 2) of 2.6 mmol/L Pi at 12 hours was concentrated and separated by SDS-PAGE along with cell lysates. C, Conditioned medium of HASMC on day 10 in the absence (lanes 1 and 3) or presence (lanes 2 and 4) of 2.6 mmol/L Pi was subjected to immunoprecipitation with anti-Gas6 antibody (lanes 1 and 2) or control goat IgG (lanes 3 and 4). Precipitates were immunoblotted with anti-Gas6 antibody. D, After pretreatment with rhGas6 (400 ng/mL) with or without Axl-ECD (1 μg/mL), apoptosis was induced by 2.6 mmol/L Pi. All values are presented as mean±SEM (n=3). *$P<0.05$ by Fisher's test. E, For measurement of Ca deposition, HASMC were cultured with rhGas6 (400 ng/mL) with or without Axl-ECD (1 μg/mL) in the presence of 2.6 mmol/L Pi for 6 days. All values are presented as mean±SEM (n=6). *$P<0.05$ by Fisher's test. Experiments were performed with at least 3 different cell populations.

Gas6 and examined the effect of atorvastatin on Pi-induced apoptosis and calcification. Transfection of Gas6 siRNA markedly decreased Gas6 expression in the short-term and long-term conditions (Figure 6A). The inhibitory effect of atorvastatin on Pi-induced apoptosis and calcification was reversed by Gas6 siRNA (Figure 6B and 6C). Similarly, the beneficial effect of atorvastatin was also abolished by blocking the binding of Gas6 to Axl using Axl-ECD (Figure 6D and 6E). These data support a critical role of Gas6 in the preventive effect of statins on apoptosis and calcification.

Discussion

The present study demonstrated that statins protected HASMC from Pi-induced calcification. The clinical effect of statins on vascular calcification is controversial. Many retrospective clinical studies[6,7,9] and a prospective study[8] have shown beneficial effects, whereas recent prospective studies were unable to show such effects.[12,13] The reason is not yet clear, and the time window of statin use has been raised as an important matter. The discrepancy may also derive from the complex in vivo effects of statins. In this regard, it is important to analyze the detailed regulatory mechanism of statins in a simple model.

In Pi-induced calcification, HASMC undergo apoptosis. A causal link between apoptosis and calcification was evident from the finding that both apoptosis and calcification were inhibited by the general caspase inhibitor, ZVAD.fmk. As reported previously,[25] we confirmed that NPC-mediated Pi uptake is another essential mechanism for HASMC calcification. Given that apoptosis does not always lead to calcification, Pi-induced HASMC calcification is presumably dependent on both an NPC-mediated phenotypic transition from SMC to an osteoblastic phenotype and apoptotic cell death. With respect to the mechanism of action of statins, they clearly inhibited Pi-induced apoptosis, although they did not have an effect on Pi-induced NPC activity or osteoblastic differentiation; Pi-induced upregulation of matrix Gla protein (MGP) mRNA was not inhibited by atorvastatin (supplemental Figure VI). These results suggest that apoptosis is the target of statins in inhibiting HASMC calcification.

Another important signal in Pi-induced calcification is an increase in intracellular Ca ($[Ca^{2+}]_i$). Statins have been shown to inhibit VSMC proliferation[5] and reduce the acute increase of $[Ca^{2+}]_i$ in a mevalonate and isoprenoid pathway–independent manner.[26] On the other hand, $[Ca^{2+}]_i$ is reported to modulate Pi-induced apoptosis of terminally differentiated chondrocytes.[27] Therefore, modulation of $[Ca^{2+}]_i$ is another possible mechanism of the inhibition of apoptosis by statins. In this study, we investigated the association of proliferation with Pi-induced apoptosis and calcification. We found that Pi did not affect proliferation, measured by the incorporation of 5-bromo-2′-deoxyuridine (BrdU) during calcification (data not shown). We also found that the inhibitory effect of statins on calcification was not affected by an inhibitor of Rho kinase (Y-27632), an important modulator of the mevalonate and isoprenoid pathway affecting proliferation and apoptosis (supplemental Figure VII). These results suggest that proliferation is not associated with Pi-induced calcification. The inhibitory effect of statins on calcification was not blocked by mevalonate, farnesylpyrophosphate, geranylgeranylpyrophosphate, or Rho kinase inhibitor, suggesting that the effect of statins is not dependent on the mevalonate and isoprenoid pathways. Indeed, a mevalonate pathway–independent effect of statins has been reported previously,[26,28–30] although the precise mechanism has not been shown. The pleiotropism of statins is of continuing interest.

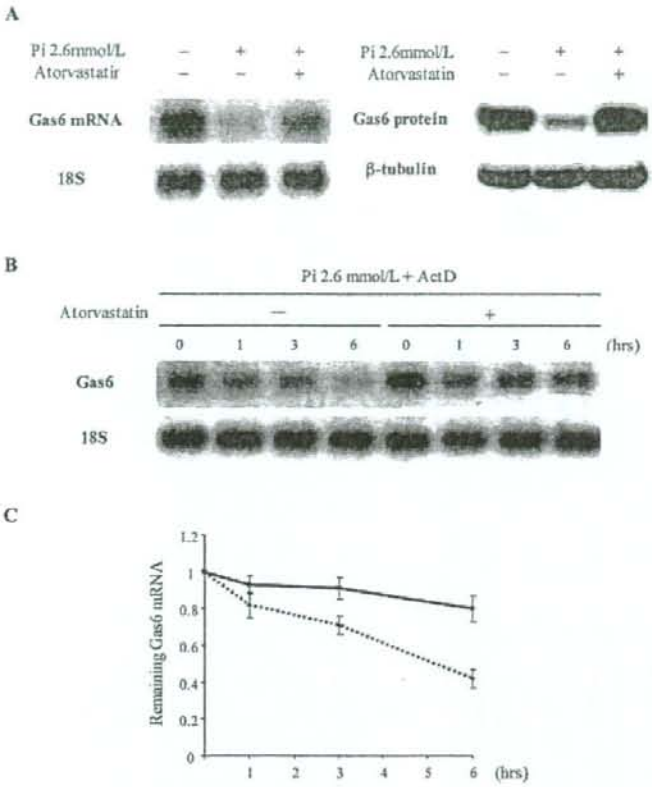

Figure 5. Atorvastatin enhances Gas6 mRNA stabilization, but not transcription. A, After pretreatment with atorvastatin (0.1 μmol/L) for 12 hours, apoptosis was induced by 2.6 mmol/L Pi. At 12 hours, mRNA was isolated and Northern blot analysis for Gas6 and 18S was performed. Simultaneously, cell lysates were collected and subjected to SDS-PAGE followed by immunoblotting with antibodies to Gas6 and β-tubulin. B, Serum-starved HASMC were incubated with actinomycin D (Act D) (5 μg/mL) in the presence of 2.6 mmol/L Pi after 12 hours of atorvastatin (0.1 μmol/L) treatment. Total RNA was harvested at 0, 1, 3, and 6 hours for Northern blot analysis. C, Signal density of Gas6 mRNA with (solid line) or without (dotted line) atorvastatin (0.1 μmol/L) in the presence of 2.6 mmol/L Pi and Act D (5 μg/mL) was normalized to that of 18S RNA at each time point. Gas6 mRNA level at time 0 was given the value 1. Each experiment was performed in triplicate for each condition.

An antiapoptotic effect of statins has been shown in various cell types.[31–34] In cardiomyocytes, apoptosis induced by hypoxia or protein kinase C (PKC) inhibitors was inhibited by 10 μmol/L pravastatin or 0.1 μg/mL atorvastatin, respectively.[31,32] Simvastatin (1 μmol/L) promoted endothelial cell survival.[33] In VSMC, 7-ketocholesterol–induced apoptosis was inhibited by 10 μmol/L pravastatin.[34] However, in contrast to the results of the present and other studies, a proapoptotic effect of statins has also been reported in VSMC,[35] endothelial cells,[36] and cardiac myocytes.[37] Although the precise mechanism is not understood, it can be postulated that statins have biphasic effects on cell survival (an antiapoptotic effect at low concentrations and a proapoptotic effect at high concentrations) depending on the type of cell, statins, and apoptotic stimulus. Indeed, Weis et al showed dose-dependent biphasic effects of statins on apoptotic activity in microvascular endothelial cells.[30] Consistent with these data, we found that 3 different statins displayed an antiapoptotic effect at low concentrations and a proapoptotic effect at high concentrations (>1 μmol/L for atorvastatin and fluvastatin; >100 μmol/L for pravastatin) (data not shown).

During Pi-induced apoptosis, we have shown that Pi downregulates the Gas6-Axl interaction, resulting in blockade of a survival signal, thereby promoting apoptosis and calcification. We previously proposed that Gas6 may allow Axl-expressing phagocytic cells, eg, macrophages and VSMC, to recognize cells exposing phosphatidylserine (PS) on the outer cell membrane, the initial step of the apoptotic process.[38] Proudfoot et al also showed that in vascular calcification, several PS-exposing cells are observed within and on the periphery of the nodules.[16] PS exposure by apoptotic bodies generates a potential Ca-binding site and membrane surface suitable for hydroxyapatite deposition.[39,40] Based on these observations, Gas6-Axl downregulation is presumably involved in decreased cell survival and clearance, both directing cells to apoptosis-mediated mineral deposition.

With regard to the molecular pathway of the restoration of Gas6 by statins, we have shown that statins retarded degradation of Gas6 mRNA, not increasing the transcriptional rate. Indeed, it was reported that statins improve mRNA stability as well as transcription.[41,42] In addition, the result that suppression of the action of Gas6 by siRNA and Axl-ECD abrogated the inhibitory effect of statins on apoptosis and inhibition clearly indicates a pivotal role of Gas6 in the effect of statins.

We conclude that statins inhibit Pi-induced HASMC calcification by preventing apoptosis via restoration of the Gas6-Axl pathway. The regulation of Gas6 by statins occurs at the posttranscriptional level. The present study provides evidence of a preventive role of statins in vascular calcification and further indicates the pleiotropic effects of statins, which could potentially contribute to the treatment of cardiovascular disease.

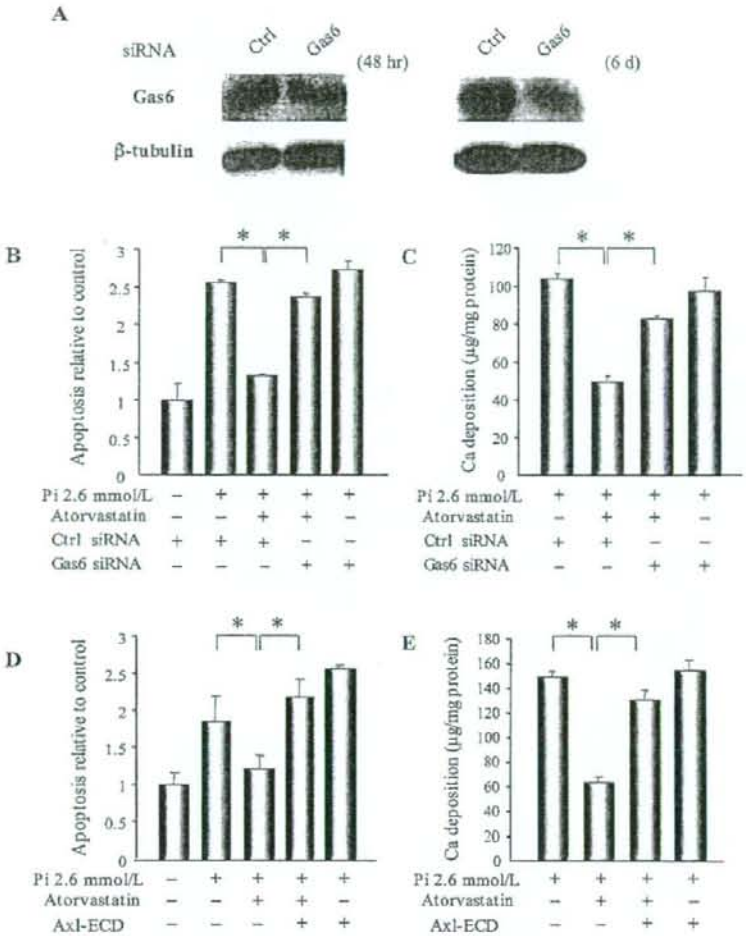

Figure 6. Gas6 knockdown abolishes inhibition of Pi-induced apoptosis and calcification by atorvastatin. A, Gas6-specific siRNA (100 nmol/L) and nonspecific siRNA (Ctrl siRNA) were transfected into HASMC, and immunoblotting was performed at 48 hours and 6 days after transfection. B, Serum-starved HASMC were transfected with 100 nmol/L Gas6 siRNA and control (Ctrl) siRNA. After transfection, cells were treated with atorvastatin (0.1 μmol/L) for 12 hours, then with 2.6 mmol/L Pi for an additional 24 hours before measurement of apoptosis (n=3). C, For measurement of Ca deposition, HASMC were transfected with 100 nmol/L Gas6 siRNA and control siRNA and incubated with atorvastatin (0.1 μmol/L) and 2.6 mmol/L Pi for 6 days (n=3). D, In the case of Axl-ECD, HASMC were pretreated with atorvastatin (0.1 μmol/L) and Axl-ECD (1 μg/mL) for 12 hours, then incubated with 2.6 mmol/L Pi for an additional 24 hours. Thereafter, a quantitative index of apoptosis was determined by ELISA (n=3). E, HASMC were cultured with atorvastatin (0.1 μmol/L) and Axl-ECD (1 μg/mL) in the presence of 2.6 mmol/L Pi for 6 days. Ca content was measured and normalized by cell protein content. All values are presented as mean±SEM (n=6). *$P<0.05$ by Fisher's test. Each panel shows a representative example of 3 independent experiments.

Acknowledgments

This study was supported by a grant-in-aid for scientific research from the Ministry of Education, Science, Sports, and Culture of Japan (grant 15390239) and by the Mitsui Sumitomo Insurance Welfare Foundation, the Ono Medical Research Foundation, the Kanzawa Medical Research Foundation, the Novartis Foundation for Gerontrogical Research, and the Takeda Research Foundation. We thank Yuki Ito for technical assistance.

References

1. Eggen DA. Relationship of calcified lesions to clinically significant atherosclerotic lesions. *Ann N Y Acad Sci.* 1968;149:752–767.
2. Wexler L, Brundage B, Crouse J, Detrano R, Fuster V, Maddahi J, Rumberger J, Stanford W, White R, Taubert K. Coronary artery calcification: pathophysiology, epidemiology, imaging methods, and clinical implications. A statement for health professionals from the American Heart Association Writing Group. *Circulation.* 1996;94:1175–1192.
3. Mullen MJ, Wright D, Donald AE, Thorne S, Thomson H, Deanfield JE. Atorvastatin but not L-arginine improves endothelial function in type-I diabetes mellitus: a double-blind study. *J Am Coll Cardiol.* 2000;36:410–416.
4. Bustos C, Hernandez-Presa MA, Ortego M, Tunon J, Ortega L, Perez F, Diaz C, Hernandez G, Egido J. HMG-CoA reductase inhibition by atorvastatin reduces neointimal inflammation in a rabbit model of atherosclerosis. *J Am Coll Cardiol.* 1998;32:2057–2064.
5. Axel DI, Riessen R, Runge H, Viebahn R, Karsch KR. Effects of cerivastatin on human arterial smooth muscle cell proliferation and migration in transfilter cocultures. *J Cardiovasc Pharmacol.* 2000;35:619–629.
6. Shavelle DM, Takasu J, Budoff MJ, Mao S, Zhao XQ, O'Brien KD. HMG CoA reductase inhibitor (statin) and aortic valve calcium. *Lancet.* 2002;359:1125–1126.
7. Novaro GM, Tiong IY, Pearce GL, Lauer MS, Sprecher DL, Griffin BP. Effect of hydroxymethylglutaryl coenzyme A reductase inhibitors on the progression of calcific aortic stenosis. *Circulation.* 2001;104:2205–2209.
8. Achenbach S, Ropers D, Pohle K, Leber A, Thilo C, Knez A, Menendez T, Maeffert R, Kusus M, Regenfus M, Bickel A, Haberl R, Steinbeck G, Moshage W, Daniel WG. Influence of lipid-lowering therapy on the progression of coronary artery calcification: a prospective evaluation. *Circulation.* 2002;106:1077–1082.
9. Callister TQ, Raggi P, Cooil B, Lippolis NJ, Russo DJ. Effect of HMG-CoA reductase inhibitors on coronary artery disease as assessed by electron-beam computed tomography. *N Engl J Med.* 1998;339:1972–1978.
10. Williams JK, Sukhova GK, Herrington DM, Libby P. Pravastatin has cholesterol-lowering independent effects on the artery wall of atherosclerotic monkeys. *J Am Coll Cardiol.* 1998;31:684–691.
11. Bea F, Blessing E, Bennett B, Levitz M, Wallace EP, Rosenfeld ME. Simvastatin promotes atherosclerotic plaque stability in apoE-deficient mice independently of lipid lowering. *Arterioscler Thromb Vasc Biol.* 2002;22:1832–1837.
12. Cowell SJ, Newby DE, Prescott RJ, Bloomfield P, Reid J, Northridge DB, Boon NA. A randomized trial of intensive lipid-lowering therapy in calcific aortic stenosis. *N Engl J Med.* 2005;352:2389–2397.

13. Wanner C, Krane V, Marz W, Olschewski M, Mann JF, Ruf G, Ritz E. Atorvastatin in patients with type 2 diabetes mellitus undergoing hemodialysis. *N Engl J Med.* 2005;353:238–248.
14. Goodman WG, London G, Amann K, Block GA, Giachelli C, Hruska KA, Ketteler M, Levin A, Massy Z, McCarron DA, Raggi P, Shanahan CM, Yorioka N; Vascular Calcification Work Group. Vascular calcification in chronic kidney disease. *Am J Kidney Dis.* 2004;43:572–579.
15. Giachelli CM, Jono S, Shioi A, Nishizawa Y, Mori K, Morii H. Vascular calcification and inorganic phosphate. *Am J Kidney Dis.* 2001;38: S34–S37.
16. Proudfoot D, Skepper JN, Hegyi L, Bennett MR, Shanahan CM, Weissberg PL. Apoptosis regulates human vascular calcification by apoptotic bodies. *Circ Res.* 2000;87:1055–1062.
17. Mansfield K, Rajpurohit R, Shapiro IM. Extracellular phosphate ions cause apoptosis of terminally differentiated epiphyseal chondrocytes. *J Cell Physiol.* 1999;179:276–286.
18. Collett G, Wood A, Alexander MY, Varnum BC, Boot-Handford RP, Ohanian V, Ohanian J, Fridell YW, Canfield AE. Receptor tyrosine kinase Axl modulates the osteogenic differentiation of pericytes. *Circ Res.* 2003;92:1123–1129.
19. Mark MR, Chen J, Hammonds RG, Sadick M, Godowski PJ. Characterization of Gas6, a member of the superfamily of G domain-containing proteins, as a ligand for Rse and Axl. *J Biol Chem.* 1996;271:9785–9789.
20. Yanagita M, Arai H, Ishii K, Nakano T, Ohashi K, Mizuno K, Varnum B, Fukatsu A, Doi T, Kita T. Gas6 regulates mesangial cell proliferation through Axl in experimental glomerulonephritis. *Am J Pathol.* 2001;158: 1423–1432.
21. Goruppi S, Ruaro E, Schneider C. Gas6, the ligand of Axl tyrosine kinase receptor, has mitogenic and survival activities for serum starved NIH3T3 fibroblasts. *Oncogene.* 1996;12:471–480.
22. Nakano T, Ishimoto Y, Kishino J, Umeda M, Inoue K, Nagata K, Ohashi K, Mizuno K, Arita H. Cell adhesion to phosphatidylserine mediated by a product of growth arrest-specific gene 6. *J Biol Chem.* 1997;272: 29411–29414.
23. Fridell YW, Villa J Jr, Attar EC, Liu ET. Gas6 induces Axl-mediated chemotaxis of vascular smooth muscle cells. *J Biol Chem.* 1998;273: 7123–7126.
24. Ming Cao W, Murao K, Imachi H, Sato M, Nakano T, Kodama T, Sasaguri Y, Wong NC, Takahara J, Ishida T. Phosphatidylinositol 3-OH kinase-Akt/protein kinase B pathway mediates Gas6 induction of scavenger receptor a in immortalized human vascular smooth muscle cell line. *Arterioscler Thromb Vasc Biol.* 2001;21:1592–1597.
25. Jono S, McKee MD, Murry CE, Shioi A, Nishizawa Y, Mori K, Morii H, Giachelli CM. Phosphate regulation of vascular smooth muscle cell calcification. *Circ Res.* 2000;87:e10–e17.
26. Bergdahl A, Persson E, Hellstrand P, Sward K. Lovastatin induces relaxation and inhibits L-type Ca(2+) current in the rat basilar artery. *Pharmacol Toxicol.* 2003;93:128–134.
27. Mansfield K, Pucci B, Adams CS, Shapiro IM. Induction of apoptosis in skeletal tissues: phosphate-mediated chick chondrocyte apoptosis is calcium dependent. *Calcif Tissue Int.* 2003;73:161–172.
28. Weitz-Schmidt G, Welzenbach K, Brinkmann V, Kamata T, Kallen J, Bruns C, Cottens S, Takada Y, Hommel U. Statins selectively inhibit leukocyte function antigen-1 by binding to a novel regulatory integrin site. *Nat Med.* 2001;7:687–692.
29. Wagner AH, Gebauer M, Guldenzoph B, Hecker M. 3-Hydroxy-3-methylglutaryl coenzyme A reductase-independent inhibition of CD40 expression by atorvastatin in human endothelial cells. *Arterioscler Thromb Vasc Biol.* 2002;22:1784–1789.
30. Weis M, Heeschen C, Glassford AJ, Cooke JP. Statins have biphasic effects on angiogenesis. *Circulation.* 2002;105:739–745.
31. Bergmann MW, Rechner C, Freund C, Baurand A, El Jamali A, Dietz R. Statins inhibit reoxygenation-induced cardiomyocyte apoptosis: role for glycogen synthase kinase 3β and transcription factor β-catenin. *J Mol Cell Cardiol.* 2004;37:681–690.
32. Tanaka K, Honda M, Takabatake T. Anti-apoptotic effect of atorvastatin, a 3-hydroxy-3-methylglutaryl coenzyme a reductase inhibitor, on cardiac myocytes through protein kinase C activation. *Clin Exp Pharm Phy.* 2004;31:360–364.
33. Kureishi Y, Luo Z, Shiojima I, Bialik A, Fulton D, Lefer DJ, Sessa WC, Walsh K. The HMG-CoA reductase inhibitor simvastatin activates the protein kinase Akt and promotes angiogenesis in normocholesterolemic animals. *Nature Med.* 2000;6:1004–1010.
34. Miyashita Y, Ozaki H, Koide N, Otsuka M, Oyama T, Itoh Y, Mastuzaka T, Shirai K. Oxysterol-induced apoptosis of vascular smooth muscle cells is reduced by HMG-CoA reductase inhibitor, pravastatin. *J Atheroscler Thromb.* 2002;9:65–71.
35. Guijarro C, Blanco-Colio LM, Ortego M, Alonso C, Ortiz A, Plaza JJ, Diaz C, Hernandez G, Egido J. 3-Hydroxy-3 methylglutaryl coenzyme A reductase and isoprenylation inhibitors induce apoptosis of vascular smooth muscle cells in culture. *Circ Res.* 1998;83:490–500.
36. Newton CJ, Ran G, Xie YX, Bilko D, Burgoyne CH, Adams I, Abidia A, McCollum PT, Atkin SL. Statin-induced apoptosis of vascular endothelial cells is blocked by dexamethasone. *J Endocrinol.* 2002;174:7–16.
37. Ogata Y, Takahashi M, Takeuchi K, Ueno S, Mano H, Ookawara S, Kobayashi E, Ikeda U, Shimada K. Fluvastatin induces apoptosis in rat neonatal cardiac myocytes: a possible mechanism of statin-attenuated cardiac hypertrophy. *J Cardiovasc Pharmacol.* 2002;40:907–915.
38. Ishimoto Y, Ohashi K, Mizuno K, Nakano T. Promotion of the uptake of PS liposomes and apoptotic cells by a product of growth arrest-specific gene, gas6. *J Biochem (Tokyo).* 2000;127:411–417.
39. Cotmore JM, Nichols G Jr, Wuthier RE. Phospholipid-calcium phosphate complex: enhanced calcium migration in the presence of phosphate. *Science.* 1971;172:1339–1341.
40. Skrtic D, Eanes ED. Membrane mediated precipitation of calcium phosphate in model liposomes with matrix vesicle-like lipid composition. *Bone Miner.* 1992;16:109–119.
41. Walter DH, Zeiher AM, Dimmeler S. Effects of statins on endothelium and their contribution to neovascularization by mobilization of endothelial progenitor cells. *Coron Artery Dis.* 2004;15:235–242.
42. Menschikowski M, Hagelgans A, Heyne B, Hempel U, Neumeister V, Goez P, Jaross W, Siegert G. Statins potentiate the IFN-gamma-induced upregulation of group IIA phospholipase A2 in human aortic smooth muscle cells and HepG2 hepatoma cells. *Biochim Biophys Acta.* 2005; 1733:157–171.

Available online at www.sciencedirect.com
ScienceDirect
European Journal of Pharmacology 556 (2007) 1–8
www.elsevier.com/locate/ejphar

Gas6/Axl-PI3K/Akt pathway plays a central role in the effect of statins on inorganic phosphate-induced calcification of vascular smooth muscle cells

Bo-Kyung Son [a], Koichi Kozaki [b], Katsuya Iijima [a], Masato Eto [a], Toru Nakano [c], Masahiro Akishita [a], Yasuyoshi Ouchi [a,*]

[a] *Department of Geriatric Medicine, Graduate School of Medicine, The University of Tokyo, 7-3-1 Hongo, Bunkyo-ku, Tokyo 113-8655, Japan*
[b] *Department of Geriatric Medicine, Kyorin University School of Medicine, Tokyo, Japan*
[c] *Discovery Research Laboratory, Shionogi and Co., Ltd., Osaka, Japan*

Received 19 May 2006; received in revised form 22 September 2006; accepted 27 September 2006
Available online 18 October 2006

Abstract

Apoptosis is essential for the initiation and progression of vascular calcification. Recently, we showed that *3-hydroxy-3-methylglutaryl* (HMG) CoA reductase inhibitors (statins) have a protective effect against vascular smooth muscle cell calcification by inhibiting apoptosis, where growth arrest-specific gene 6 (Gas6) plays a pivotal role. In the present study, we clarified the downstream targets of Gas6-mediated survival signaling in inorganic phosphate (Pi)-induced apoptosis and examined the effect of statins. We found that fluvastatin and pravastatin significantly inhibited Pi-induced apoptosis and calcification in a concentration-dependent manner in human aortic smooth muscle cells (HASMC), as was found with atorvastatin previously. Gas6 and its receptor, Axl, expression were downregulated in the presence of Pi, and recombinant human Gas6 (rhGas6) significantly inhibited apoptosis and calcification in a concentration-dependent manner. During apoptosis, Pi suppressed Akt phosphorylation, which was reversed by rhGas6. Wortmannin, a specific *phosphatidylinositol 3-OH kinase* (PI3K) inhibitor, abolished the increase in Akt phosphorylation by rhGas6 and eliminated the inhibitory effect of rhGas6 on both Pi-induced apoptosis and calcification, suggesting that PI3K-Akt is a downstream signal of the Gas6-mediated survival pathway. Pi reduced phosphorylation of Bcl2 and Bad, and activated caspase 3, all of which were reversed by rhGas6. The inhibitory effect of statins on Pi-induced apoptosis was accompanied by restoration of the Gas6-mediated survival signal pathway: upregulation of Gas6 and Axl expression, increased phosphorylation of Akt and Bcl2, and inhibition of Bad and caspase 3 activation. These findings indicate that the Gas6-mediated survival pathway is the target of statins' effect to prevent vascular calcification.

Keywords: Calcification; Apoptosis; Gas6; Axl; Akt; Bcl2

1. Introduction

Vascular calcification, such as coronary and aortic calcification, is clinically important in the development of cardiovascular disease (Eggen, 1968). Two distinct forms of vascular calcification are well recognized. One is medial calcification, which occurs between the cell layers of smooth muscle cells and is related to aging, diabetes and chronic renal failure (Neubauer, 1971; Goodman et al., 2000). The other is atherosclerotic calcification, which occurs in the intima during the development of atheromatous disease (Wexler et al., 1996). In diabetic patients, medial calcification has been shown to be a strong independent predictor of cardiovascular mortality (Everhart et al., 1988).

We recently demonstrated that atorvastatin prevented inorganic phosphate (Pi)-induced calcification by inhibiting apoptosis, one of the important processes regulating calcification. This was mediated by growth arrest-specific gene 6 (Gas6), a vitamin K-dependent protein (Son et al., 2006). Gas6 binds to Axl, the predominant receptor for Gas6, on the cell surface and transduces the signal by Axl autophosphorylation (Mark et al., 1996). Gas6-Axl interaction has been shown to be implicated in the regulation of multiple cellular functions (Yanagita et al., 2001; Goruppi et al., 1996; Nakano et al., 1997; Fridell et al., 1998). Especially, they are known to protect a range of cell types

* Corresponding author. Tel.: +81 3 5800 8652; fax: +81 3 5800 6530.
E-mail address: youchi-tky@umin.ac.jp (Y. Ouchi).

0014-2999/$ - see front matter © 2006 Elsevier B.V. All rights reserved.
doi:10.1016/j.ejphar.2006.09.070

from apoptotic death (Goruppi et al., 1996, 1999; Healy et al., 2001). However, the downstream targets of Gas6-mediated signaling in Pi-induced apoptosis and the effect of statins on this pathway are poorly understood.

With respect to the targets of Gas6-Axl interaction, Lee et al. (2002) showed that activation of Akt is necessary for Gas6-dependent cell survival. Akt is an important mediator of metabolic and survival responses after growth factor stimulation. Akt is activated by phosphorylation, which is performed by phosphatidylinositol 3-OH kinase (PI3K), a kinase that is activated by Gas6-Axl interaction (Lee et al., 2002; Ming Cao et al., 2001). Activation of Akt leads to downstream signaling events including those associated with mitochondrial regulators of apoptosis such as Bcl2 and Bad.

In the present study, we examined the effect of statins using two different types: lipophilic fluvastatin and hydrophilic pravastatin. We investigated the effect of statins on Pi-induced apoptosis and calcification as well as on signaling components in this process. Consequently, we found that both statins restored the Gas6-mediated survival pathway, with upregulation of the expression of Gas6 and Axl, increased phosphorylation of Akt, Bcl2 and Bad; and finally inhibition of caspase 3 activation, resulting in the prevention of apoptosis and subsequent calcification in human aortic smooth muscle cells (HASMC).

2. Materials and methods

2.1. Materials

Pravastatin and fluvastatin were supplied by Sankyo Co. Ltd. and Tanabe Seiyaku Co., Ltd., respectively. Recombinant human Gas6 (rhGas6) was prepared as described previously (Ming et al., 2001). Wortmannin was purchased from Calbiochem. All other reagents were of analytical grade.

2.2. Cell culture

HASMC were obtained from Clonetics. They were cultured in Dulbecco's modified Eagle's medium (DMEM) supplemented with 20% *fetal bovine serum* (FBS), 100 U/ml penicillin and 100 mg/ml streptomycin at 37 °C in a humidified atmosphere with 5% CO_2. HASMC were used up to passage 8 for the experiments.

2.3. Induction and quantification of calcification

For Pi-induced calcification, Pi (a mixed solution of Na_2HPO_4 and NaH_2PO_4 whose pH was adjusted to 7.4) was added to serum-supplemented DMEM to a final concentration of 2.6 mM. After the indicated incubation period, cells were decalcified with 0.6 M HCl, and Ca content in the supernatant was determined by the *o*-cresolphthalein complexone method (C-Test, WAKO). The remaining cells were solubilized in 0.1 M NaOH/0.1% *sodium dodecyl sulfate* (SDS), and cell protein content was measured by Bio-Rad protein assay. Calcification was visualized by von Kossa's method. Briefly, the cells were fixed with 4% formaldehyde and exposed to 5% aqueous $AgNO_3$.

2.4. Induction and determination of apoptosis

Two different time courses were tested to investigate Pi-induced apoptosis and examine the effect of statins, under short-term (within 24 h) and long-term (up to 10 days) conditions (Son et al., 2006).

2.4.1. TdT-mediated dUTP nick end-labeling (TUNEL) assay

TUNEL assay to detect DNA fragmentation was performed using a commercially available kit (ApopTag Plus, Chemicon). Briefly, the samples were preincubated with equilibration buffer for 10 min, and subsequently incubated with terminal deoxyribonucleotidyl transferase in the presence of digoxigenin-conjugated dUTP for 1 h at 37 °C. The reaction was terminated by incubating the samples in stopping buffer for 30 min. After 3 rinses with *phosphate-buffered saline* (PBS), a fluorescein-labeled anti-digoxigenin antibody was applied for 30 min, and the samples were rinsed 4 times with PBS. The samples were then stained, mounted with DAPI (*4′,6-diamino-2-phenylindole*)/antifade, and examined by fluorescence microscopy.

2.4.2. Detection of DNA fragmentation by ELISA

Cytoplasmic histone-associated DNA fragments were determined with a cell-death detection ELISA^{plus} kit (Roche) as a quantitative index of apoptosis. Briefly, after the cells were incubated in lysis buffer for 30 min, 20 μl of the cell lysates was used for the assay. Following addition of substrate, colorimetric change was determined as the absorbance value measured at 405 nm.

2.5. Immunoblotting

The effect of Pi and statins on the expression of Gas6 and Axl, phosphorylation of Akt, Bcl2 and Bad, and activation of caspase 3 was examined at 12 h. The collected cell lysates were applied to SDS-polyacrylamide gels under reducing conditions, and transferred to a polyvinylidene difluoride (PVDF) membrane. Immunoblot analysis was performed using specific primary antibodies: anti-Axl, anti-Gas6 (Santa Cruz Biotechnology), anti-caspase 3, anti-Akt, anti-Bcl2, anti-phospho-Akt, anti-phospho-Bcl2, anti-phospho-Bad (Cell Signaling Technology), and anti-Bad (Transduction Laboratories). After incubation with horseradish peroxidase-conjugated secondary antibodies (Amersham Pharmacia), blots were visualized by enhanced chemiluminescence and autoradiography (ECL Plus, Amersham Pharmacia). Experiments were performed with at least three different cell populations.

2.6. Statistical analysis

All results are presented as mean±S.E.M. Statistical comparisons were made by ANOVA, unless otherwise stated. A value of $P<0.05$ was considered to be significant.

3. Results

3.1. Statins inhibit Pi-induced apoptosis and calcification in HASMC

In HASMC, a high Pi level (≥2.6 mM), comparable to that of hyperphosphatemia in end-stage renal disease, significantly induced calcification. Fluvastatin showed an inhibitory effect on Pi-induced calcification at as high a concentration as 0.1 μM (26.1±2.3% of control), while pravastatin showed the degree of effect at 50 μM (27.4±3.1% of control) (Fig. 1A). An inhibitory effect on Ca deposition was also found by von Kossa's staining (Fig. 1B). Both statins prevented Pi-induced apoptosis at the same concentrations as those at which they prevented calcification (Fig. 1C). An antiapoptotic effect of statins was also observed by TUNEL assay on day 6 (Fig. 1D).

3.2. Gas6 plays an important role in Pi-induced apoptosis

In the presence of 2.6 mM Pi, the expression of Gas6 and Axl was markedly downregulated (Fig. 2A). To investigate the role of Gas6 in Pi-induced apoptosis and calcification, first, we tested whether supplementation of rhGas6 could prevent Pi-induced apoptosis. In HASMC, rhGas6 significantly inhibited Pi-induced apoptosis in a concentration-dependent manner (Fig. 2B). Furthermore, during apoptosis, activated products of caspase 3 (17 and 19 kDa) were significantly increased by 2.6 mM Pi, which was reversed by rhGas6 (Fig. 2C). Next, we examined the effect of rhGas6 on calcification. Recombinant human Gas6 significantly inhibited Pi-induced calcification on day 6 in a concentration-dependent manner (Fig. 2D), suggesting that Gas6 plays an important role in Pi-induced apoptosis and calcification.

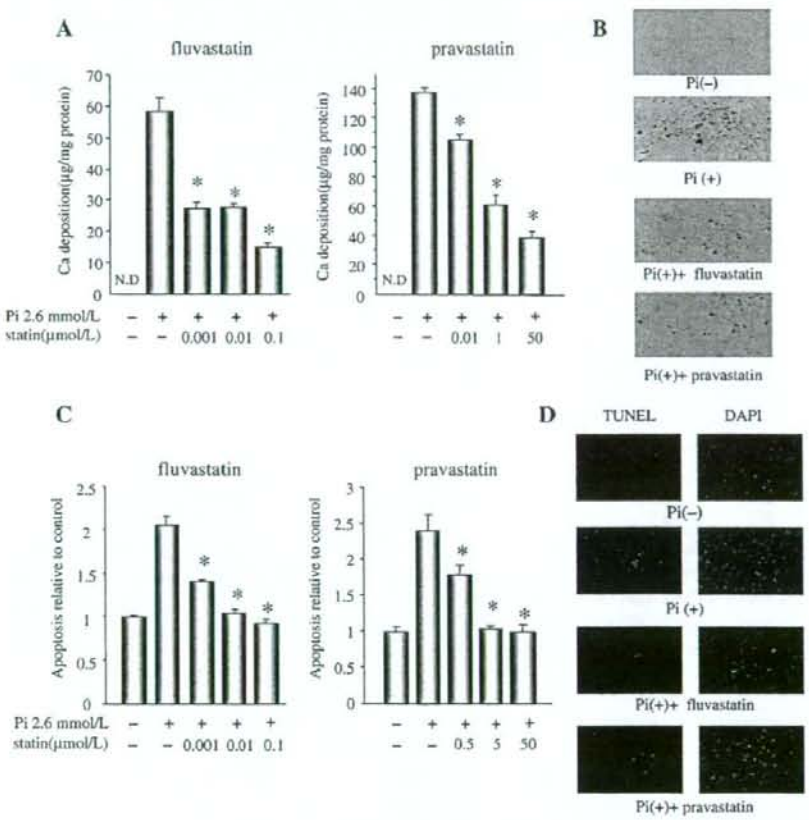

Fig. 1. Statins prevent Pi-induced apoptosis and calcification. HASMC were cultured with the indicated concentrations of fluvastatin and pravastatin in the presence of 2.6 mM Pi for 6 days. Ca deposition was measured by *o*-cresolphthalein complexone method, and normalized by cell protein content. All values are presented as mean± S.E.M. ($n=6$). *$P<0.05$ vs. statin (−) by Fisher's test. N.D. stands for "not detected" (A). On day 6, the inhibitory effect of fluvastatin (0.1 μM) and pravastatin (50 μM) on 2.6 mM Pi [Pi(+)]-induced Ca deposition was evaluated at the light microscopic level with von Kossa's staining (B). Serum-starved HASMC were cultured with the indicated concentrations of fluvastatin and pravastatin for 12 h and then incubated with 2.6 mM Pi for an additional 24 h. A quantitative index of apoptosis, determined by ELISA, is presented as the relative value to that without statins and 2.6 mM Pi. All values are presented as mean± S.E.M. ($n=3$). *$P<0.05$ vs. 2.6 mM Pi, statin (−) by Fisher's test (C). The antiapoptotic effect of fluvastatin (0.1 μM) and pravastatin (50 μM) was evaluated by TUNEL staining (green) on day 6. Nuclei were counterstained with DAPI (4′,6-diamino-2-phenylindole, blue) (D).

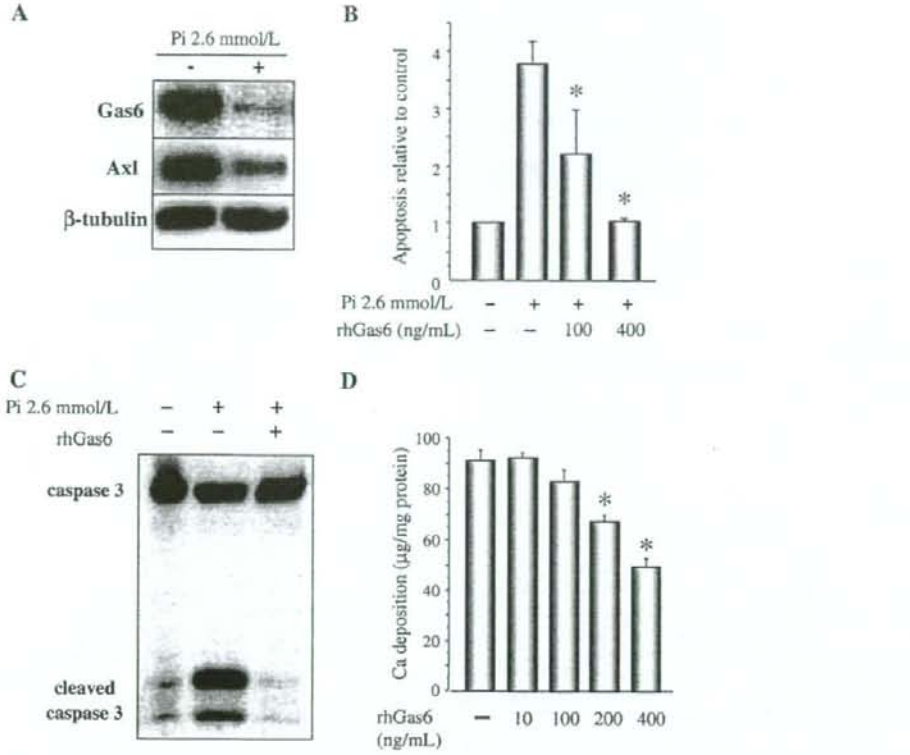

Fig. 2. Pi suppresses Gas6 and Axl expression, and rhGas6 inhibits caspase-dependent apoptosis and calcification. HASMC were cultured in the presence or absence of 2.6 mM Pi for 12 h. Cell lysates were collected and subjected to SDS-PAGE followed by immunoblotting with antibodies to Gas6, Axl or β-tubulin (A). After pretreatment with the indicated concentrations of rhGas6, apoptosis was induced by 2.6 mM Pi. All values are presented as mean±S.E.M. ($n=3$). $^*P<0.05$ vs. 2.6 mM Pi, rhGas6 (−) by Fisher's test (B). HASMC were pretreated with rhGas6 (400 ng/ml) for 1 h, then cultured with 2.6 mM Pi for 12 h. Cell lysates were immunoblotted with an antibody that recognizes caspase-3 (35 kDa) and the cleaved forms of caspase-3 (17 and 19 kDa) (C). For measurement of Ca deposition, HASMC were cultured with the indicated concentrations of rhGas6 in the presence of 2.6 mM Pi for 6 days. All values are presented as mean±S.E.M. ($n=6$). $^*P<0.05$ by Fisher's test (D). Experiments were performed with at least three different cell populations.

3.3. Downregulation of phospho-Akt participates in Pi-induced apoptosis

Since in NIH-3T3 fibroblasts, the antiapoptotic effect of Gas6-Axl interaction has been shown to be mediated by Akt phosphorylation (Goruppi et al., 1999), we examined whether Akt participates in the signaling of downregulation of the Gas6-Axl interaction during Pi-induced apoptosis. In the presence of 2.6 mM Pi, Akt phosphorylation was downregulated in a time-dependent manner, whereas the expression of total Akt was not changed (Fig. 3A). In addition, rhGas6 abrogated the Pi-induced decrease in Akt phosphorylation, implying that subsequent downregulation of Akt phosphorylation is the pathway of Pi-induced apoptosis (Fig. 3B).

Because Akt phosphorylation is regulated by PI3K, we examined the effect of wortmannin, a specific PI3K inhibitor, on rhGas6-mediated phosphorylation of Akt. As shown in Fig. 3B, wortmannin abrogated the rhGas6-induced phosphorylation of Akt and further eliminated the inhibitory effect of rhGas6 on Pi-induced apoptosis and calcification (Fig. 3C, D). These results indicate that the preventive effect of rhGas6 on Pi-induced apoptosis and calcification was mediated by the PI3K-Akt pathway.

3.4. Pi suppresses Bcl2 phosphorylation and activates Bad

To establish the downstream components of Pi-induced apoptosis, two key apoptosis-regulating proteins, Bcl2 and Bad, were analyzed. During apoptosis, phosphorylation of Bcl2 (active form) and Bad (inactive form) was markedly reduced by 2.6 mM Pi in a time-dependent manner. The expression level of their total protein was not changed in this period (Fig. 4A, B). By supplementation of the medium with rhGas6, the decrease in phosphorylation of Bcl2 and Bad by Pi was reversed to almost the basal level (Fig. 4C, D). These results indicate that Pi promotes apoptosis by inactivating Bcl2 and activating Bad via a Gas6-dependent pathway.

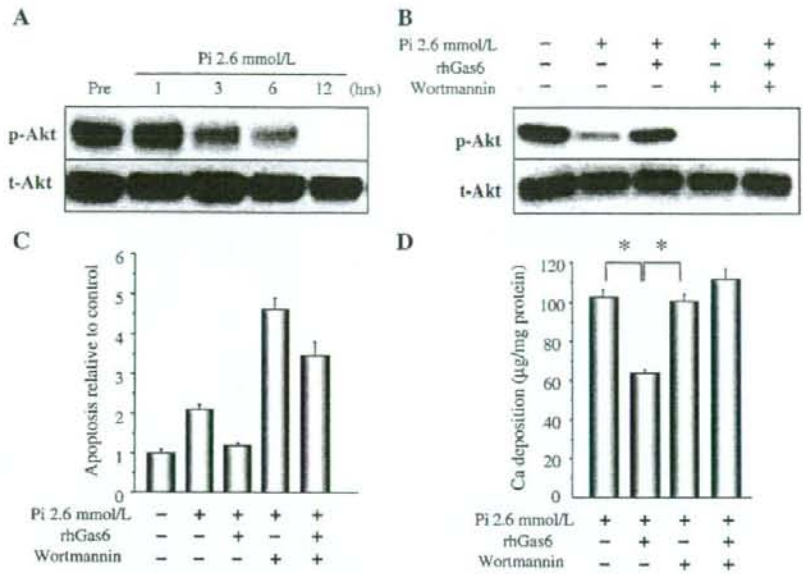

Fig. 3. Pi decreases Akt phosphorylation, and wortmannin abrogates the inhibitory effect of rhGas6 on Akt phosphorylation, apoptosis and calcification. HASMC were cultured in the presence of 2.6 mM Pi for the indicated periods. Cell lysates were immunoblotted with anti-phospho-Akt (p-Akt) antibody and total Akt (t-Akt) antibody (A). HASMC were pretreated with rhGas6 (400 ng/ml), wortmannin (1 μM), or both for 1 h, and then treated with 2.6 mM Pi for 12 h. Cell lysates were immunoblotted with p-Akt and t-Akt antibody (B). After pretreatment with rhGas6 (400 ng/ml) and wortmannin (1 μM), apoptosis was induced by 2.6 mM Pi. All values are presented as mean ± S.E.M. ($n=3$). $^*P<0.05$ vs. 2.6 mM Pi, rhGas6 (−), wortmannin (−) by Fisher's test (C). HASMC were cultured with rhGas6 (400 ng/ml) and with or without wortmannin (1 μM) in the presence of 2.6 mM Pi for 6 days. Ca content was measured and normalized by cell protein content. All values are presented as mean ± S.E.M. ($n=6$). $^*P<0.05$ by Fisher's test (D).

3.5. Gas6-mediated survival pathway is the target of statins' effect on apoptosis

To investigate whether the antiapoptotic effect of statins is associated with the Gas6-mediated survival pathway, first, we examined the effect of statins on the expression of Gas6 and Axl. As shown in Fig. 5A and B, both fluvastatin and pravastatin restored the expression of Gas6 and Axl, which was downregulated by 2.6 mM Pi. Because we have shown that the Gas6-mediated survival pathway is Akt-dependent, the effect of statins on Akt phosphorylation was examined. The Pi-induced decrease in Akt phosphorylation was restored by both statins, while total Akt expression was not changed. In addition, we found that both statins stimulated phosphorylation of Bcl2 and

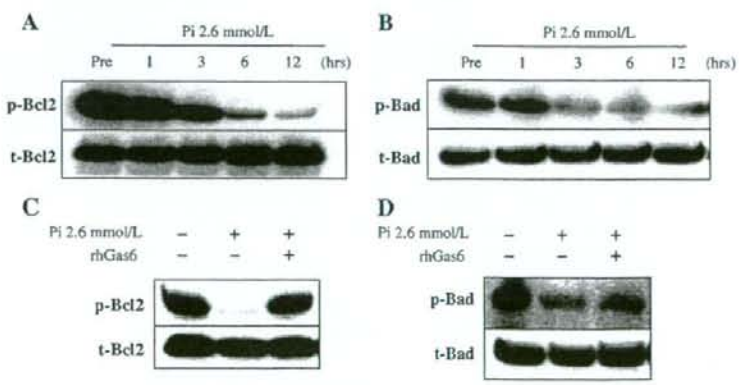

Fig. 4. RhGas6 restores Pi-induced decrease in phosphorylation of Bcl2 and Bad. HASMC were exposed to 2.6 mM Pi for the indicated periods, and cell lysates were subjected to immunoblotting with anti-phospho-Bcl2 (p-Bcl2) antibody and total Bcl2 (t-Bcl2) antibody (A), or with anti-phospho-Bad (p-Bad) antibody and total Bad (t-Bad) antibody (B). HASMC were pretreated with rhGas6 (400 ng/ml) for 1 h, and then treated with 2.6 mM Pi for 12 h. Cell lysates were subjected to immunoblotting with p-Bcl2 and t-Bcl2 antibody (C), or with p-Bad and t-Bad antibody (D).

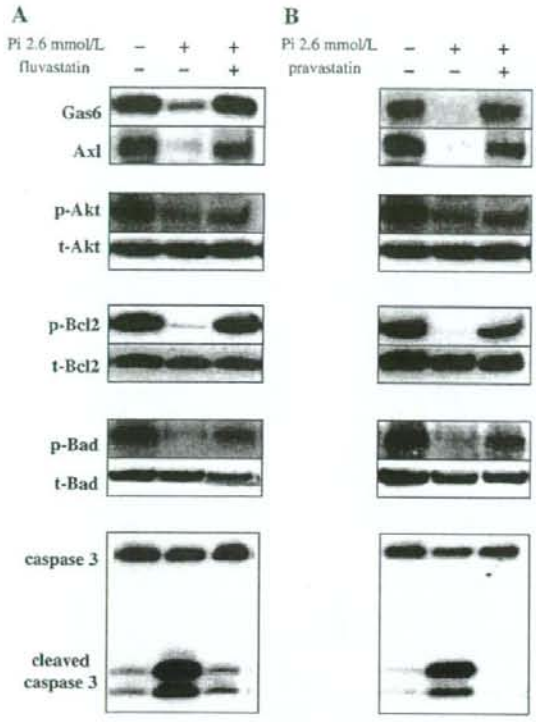

Fig. 5. Antiapoptotic effect of statins is associated with upregulation of Gas6-Axl survival pathway. After pretreatment with 0.1 μM fluvastatin (A) and 50 μM pravastatin (B) for 12 h, apoptosis was induced by 2.6 mM Pi. After 12 h, cell lysates were collected and subjected to SDS-PAGE followed by immunoblotting with antibodies that recognize Gas6 and Axl, with phospho-specific Akt (p-Akt) and total Akt (t-Akt) antibody, with phospho-specific Bcl2 (p-Bcl2) and total Bcl2 (t-Bcl2) antibody, or with phospho-specific Bad (p-Bad) and total Bad (t-Bad) antibody. Cell lysates were immunoblotted with an antibody that recognizes uncleaved caspase-3 (35 kDa) and the cleaved forms of caspase-3 (17 and 19 kDa).

Bad, with total expression unchanged. Pi-induced caspase 3 activation was also prevented by both statins. Taken together, these findings suggest that the inhibitory effect of statins on Pi-induced apoptosis is mediated by restoration of the Gas6-mediated survival pathway; PI3K-induced Akt phosphorylation, Bcl2 activation, Bad inactivation, and caspase 3 inactivation.

4. Discussion

In the present study, we found that both lipophilic fluvastatin and hydrophilic pravastatin protected against Pi-induced apoptosis and calcification in HASMC, as we found with atorvastatin previously. With regard to the different potency of statins, we found that the inhibitory effect of pravastatin was inferior to those of fluvastatin and atorvastatin, which exerted similar effects on calcification and apoptosis. This might relate to our previous finding that the inhibition of calcification by statins was not dependent on the mevalonate pathway (Son et al., 2006). Consequently, the inhibitory effect on calcification was not parallel to the cholesterol-lowering effect. We speculate that the difference between statins was derived from their affinity to *vascular smooth muscle cells* (VSMC), that is, lipophilic statins have stronger effects on VSMC calcification than hydrophilic statins.

The antiapoptotic effect of statins was induced by restoration of the Gas6-mediated survival pathway: PI3K-induced Akt phosphorylation, Bcl2 and Bad phosphorylation, and caspase 3 inactivation. Gas6 plays a crucial role in the effect of statins on Pi-induced apoptosis. Gas6, a secreted vitamin K-dependent protein, binds to the receptors of the mammalian Axl protein-tyrosine kinase family; Axl, Sky, and Mer, with different affinities (Nagata et al., 1996). Gas6 and Axl have been shown to localize in the neointima of the artery after balloon injury, in which they presumably modulate several cell functions such as differentiation, adhesion, migration, proliferation, and survival in a cell-specific manner (Melaragno et al., 1998). The Gas6-Axl interaction is also shown to upregulate scavenger receptor A expression in VSMC (Ming et al., 2001), and facilitates the clearance of apoptotic cells by macrophages (Ishimoto et al., 2000). Of the above functions, protection against apoptotic cell death has been most studied (Goruppi et al., 1996; Healy et al., 2001; Lee et al., 2002; Nakano et al., 1996). Consistently, the expression of Gas6 and Axl was downregulated by Pi, leading to apoptosis and subsequent calcification.

Several intracellular signaling pathways mediated by Gas6-Axl interaction have been shown previously (Goruppi et al., 1999; Lee et al., 2002; Ming et al., 2001). Akt, which is necessary for Gas6-dependent survival, is a critical downstream effector of the PI3K-dependent antiapoptotic pathway. In VSMC, it has been reported that the PI3K-Akt pathway mediates Gas6 induction of scavenger receptor A (Ming et al., 2001). Consistent with these reports, our study provides evidence that the PI3K-Akt pathway is a target of Gas6-Axl interaction, and downregulation of Akt phosphorylation is associated with Pi-induced apoptosis and calcification. Moreover, it is known that PI3K-Akt affects the cell death program through the Bcl2 family of proteins. This protein family is a critical regulator of apoptosis in a variety of cell types, and the balance of antiapoptotic members, such as Bcl2, versus proapoptotic mediators, such as Bad, determines cell fate (Reed, 1997). Bcl2, whose phosphorylation is required for its anti-apoptotic activity (Ruvolo et al., 2001), inhibits programmed cell death by several mechanisms: It binds to caspase CED-4 (Apaf-1) and prevents the cell execution cascade; Bcl2 alters mitochondrial membrane potential and inhibits the release of cytochrome c. On the other hand, Bad plays a proapoptotic role in its dephosphorylated form by binding to Bcl2 and reversing its anti-apoptotic effect; phosphorylation of Bad results in its cytosolic sequestration by 14-3-3 and hampers its binding to Bcl2 (Zha et al., 1996). It was also reported that Bad is directly phosphorylated by PI3K-Akt (del Peso et al., 1997). In the present study, Bcl2 was inactivated and Bad was activated (both proteins were dephosphorylated) by Pi, directing the cells to apoptosis, and rhGas6 restored phosphorylation of Bcl2 and Bad. During apoptosis, one of the final biochemical events leading to programmed

cell death is activation of the caspase cascade. Activation of caspase 3 is required for internucleosomal DNA degradation (Woo et al., 1998), and caspase inhibition prevents the release of apoptotic bodies from cells (Zhang et al., 1999). In the present study, supplementation of the medium with rhGas6 prevented Pi-induced caspase 3 activation. These results clearly show that Pi downregulates Gas6-Axl, decreases PI3K-mediated Akt phosphorylation, inactivates Bcl2, activates Bad, and activates caspase 3, leading to apoptosis.

The present study demonstrated that statins restored the Gas6-mediated survival pathway. Consistent with these results, Akt phosphorylation has been reported to be an antiapoptotic mechanism of statins: pravastatin inhibited hypoxia-induced apoptosis through activation of Akt in cardiomyocytes (Bergmann et al., 2004), and simvastatin and pravastatin enhanced phosphorylation of Akt and promoted angiogenesis in endothelial cells (Kureishi et al., 2000). Recently, it was reported that statins inhibit caspase 3 activation driven by protein kinase C inhibitors in the process of apoptosis, suggesting that caspase 3 is also under the control of statins during apoptosis (Tanaka et al., 2004).

In this study, we performed experiments under both short-term (within 24 h) and long-term (up to 10 days) conditions. In general, short-term experiments are able to examine acute cell behavior, such as signaling and transcription. However, because obvious HASMC calcification takes at least 3 days, we also performed long-term experiments. Downregulation of Gas6, Axl expression and reduced phosphorylation of Akt, Bcl2, and Bad, and a beneficial effect of statins were consistently found in the long-term condition. This confirms that the Gas6-Axl survival signal is the key mechanism for Pi-induced calcification.

It is concluded that statins inhibit Pi-induced apoptosis via the Gas6/Axl-PI3K-Akt signal pathway, which has a crucial role in the prevention of HASMC calcification. This study adds further evidence of the pleiotropic effects of statins, suggesting a therapeutic strategy for the prevention of vascular calcification.

Acknowledgements

This study was supported by a Grant-in-Aid for Scientific Research from the Ministry of Education, Science, Sports, and Culture of Japan (No. 15390239), Mitsui Sumitomo Insurance Welfare Foundation, Ono Medical Research Foundation, Kanzawa Medical Research Foundation, Novartis Foundation for Gerontological Research, and Takeda Research Foundation. We thank Yuki Ito for technical assistance.

References

Bergmann, M.W., Rechner, C., Freund, C., Baurand, A., Jamali, A., Dietz, R., 2004. Statins inhibit reoxygenation-induced cardiomyocyte apoptosis: role for glycogen synthase kinase 3β and transcription factor β-catenin. J. Mol. Cell. Cardiol. 37, 681–690.

del Peso, L., Gonzalez-Garcia, M., Page, C., Herrera, R., Nunez, G., 1997. Interleukin-3-induced phosphorylation of Bad through protein kinase Akt. Science 278, 687–689.

Eggen, D.A., 1968. Relationship of calcified lesions to clinically significant atherosclerotic lesions. Ann. N. Y. Acad. Sci. 149, 752–767.

Everhart, J.E., Pettitt, D.J., Knowler, W.C., Rose, F.A., Bennett, P.H., 1988. Medial artery calcification and its association with mortality and complications of diabetes. Diabetologia 31, 16–23.

Fridell, Y.W., Villa Jr., J., Attar, E.C., Liu, E.T., 1998. Gas6 induces Axl-mediated chemotaxis of vascular smooth muscle cells. J. Biol. Chem. 273, 7123–7126.

Goodman, W.G., Goldin, J., Kuizon, B.D., Yoon, C., Gales, B., Sider, D., Wang, Y., Chung, J., Emerick, A., Greaser, L., Elashoff, R.M., Salusky, I.B., 2000. Coronary-artery calcification in young adults with end-stage renal disease who are undergoing dialysis. N. Engl. J. Med. 342, 1478–1483.

Goruppi, S., Ruaro, E., Schneider, C., 1996. Gas6, the ligand of Axl tyrosine kinase receptor, has mitogenic and survival activities for serum starved NIH3T3 fibroblasts. Oncogene 12, 471–480.

Goruppi, S., Ruaro, E., Varnum, B., Schneider, C., 1999. Gas6-mediated survival in NIH3T3 cells activates stress signaling cascade and is independent of Ras. Oncogene 18, 4224–4236.

Healy, A.M., Schwartz, J.J., Zhu, X., Herrick, B.E., Varnum, B., Farber, H.W., 2001. Gas6 promotes Axl-mediated survival in pulmonary endothelial cells. Am. J. Physiol., Lung Cell. Mol. Physiol 280, L1273–L1281.

Ishimoto, Y., Ohashi, K., Mizuno, K., Nakano, T., 2000. Promotion of the uptake of PS liposomes and apoptotic cells by a product of growth arrest-specific gene, gas6. J. Biochem. (Tokyo) 127, 411–417.

Kureishi, Y., Luo, Z., Shiojima, I., Bialik, A., Fulton, D., Lefer, D.J., Sessa, W.C., Walsh, K., 2000. The HMG-CoA reductase inhibitor simvastatin activates the protein kinase Akt and promotes angiogenesis in normocholesterolemic animals. Nat. Med. 6, 1004–1010.

Lee, W.P., Wen, Y., Varnum, B., Hung, M.C., 2002. Akt is required for Axl-Gas6 signaling to protect cells from E1A-mediated apoptosis. Oncogene 21, 329–336.

Mark, M.R., Chen, J., Hammonds, R.G., Sadick, M., Godowsk, P.J., 1996. Characterization of Gas6, a member of the superfamily of G domain-containing proteins, as a ligand for Rse and Axl. J. Biol. Chem. 271, 9785–9789.

Melaragno, M.G., Wuthrich, D.A., Poppa, V., Gill, D., Lindner, V., Berk, B.C., Corson, M.A., 1998. Increased expression of Axl tyrosine kinase after vascular injury and regulation by G protein-coupled receptor agonists in rats. Circ. Res. 83, 697–704.

Ming Cao, W., Murao, K., Imachi, H., Sato, M., Nakano, T., Kodama, T., Sasaguri, Y., Wong, N.C., Takahara, J., Ishida, T., 2001. Phosphatidylinositol 3-OH kinase-Akt/protein kinase B pathway mediates Gas6 induction of scavenger receptor a in immortalized human vascular smooth muscle cell line. Arterioscler. Thromb. Vasc. Biol. 21, 1592–1597.

Nagata, K., Ohashi, K., Nakano, T., Arita, H., Zong, C., Hanafusa, H., Mizuno, K., 1996. Identification of the product of growth arrest-specific gene 6 as a common ligand for Axl, Sky, and Mer receptor tyrosine kinases. J. Biol. Chem. 271, 30022–30027.

Nakano, T., Kawamoto, K., Higashino, K., Arita, H., 1996. Prevention of growth-arrest induced cell death of vascular smooth muscle cells by a product of growth arrest-specific gene, gas6. FEBS Lett. 387, 78–80.

Nakano, T., Ishimoto, Y., Kishino, J., Umeda, M., Inoue, K., Nagata, K., Ohashi, K., Mizuno, K., Arita, H., 1997. Cell adhesion to phosphatidylserine mediated by a product of growth arrest-specific gene 6. J. Biol. Chem. 272, 29411–29414.

Neubauer, B., 1971. A quantitative study of peripheral arterial calcification and glucose tolerance in elderly diabetics and non-diabetics. Diabetologia 7, 409–413.

Reed, J.C., 1997. Double identity for proteins of the Bcl-2 family. Nature 387, 773–776.

Ruvolo, P.P., Deng, X., May, W.S., 2001. Phosphorylation of Bcl2 and regulation of apoptosis. Leukemia 515–522.

Son, B.K., Kozaki, K., Iijima, K., Eto, M., Kojima, T., Ota, H., Senda, Y., Maemura, K., Nakano, T., Akishita, M., Ouchi, Y., 2006. Statins protect human aortic smooth muscle cells from inorganic phosphate-induced calcification by restoring Gas6-Axl survival pathway. Circ. Res. 98, 1024–1031.

Tanaka, K., Honda, M., Takabatake, T., 2004. Anti-apoptotic effect of atorvastatin, a 3-hydroxy-3-methylglutaryl coenzyme a reductase inhibitor, on cardiac myocytes through protein kinase C activation. Clin. Exp. Pharmacol. Physiol. 31, 360–364.

Wexler, L., Brundage, B., Crouse, J., Detrano, R., Fuster, V., Maddahi, J., Rumberger, J., Stanford, W., White, R., Taubert, K., 1996. Coronary artery calcification: pathophysiology, epidemiology, imaging methods, and clinical

implications. A statement for health professionals from the American Heart Association. Writing Group. Circulation 94, 1175–1192.

Woo, M., Hakem, R., Soengas, M.S., Duncan, G.S., Shahinian, A., Kagi, D., Hakem, A., McCurrach, M., Khoo, W., Kaufman, S.A., Senaldi, G., Howard, T., Lowe, S.W., Mak, T.W., 1998. Essential contribution of caspase3/CPP32 to apoptosis and its associated nuclear changes. Genes Dev. 12, 806–819.

Yanagita, M., Arai, H., Ishii, K., Nakano, T., Ohashi, K., Mizuno, K., Varnum, B., Fukatsu, A., Doi, T., Kita, T., 2001. Gas6 regulates mesangial cell proliferation through Axl in experimental glomerulonephritis. Am. J. Pathol. 158, 1423–1432.

Zha, J., Harada, H., Yang, E., Jockel, J., Korsmeyer, S.J., 1996. Serine phosphorylation of death agonist BAD in response to survival factor results in binding to 14-3-3 not BCL-X(L). Cell 87, 619–628.

Zhang, J., Reedy, M.C., Hannun, Y.A., Obeid, L.M., 1999. Inhibition of caspases inhibits the release of apoptotic bodies: Bcl2 inhibits the initiation of formation of apoptotic bodies in chemotherapeutic agent-induced apoptosis. J. Cell Biol. 145, 99–108.

ELSEVIER

Atherosclerosis 191 (2007) 281–289

ATHEROSCLEROSIS

www.elsevier.com/locate/atherosclerosis

Potent free radical scavenger, edaravone, suppresses oxidative stress-induced endothelial damage and early atherosclerosis

Hang Xi[a], Masahiro Akishita[b,*], Kumiko Nagai[a], Wei Yu[a], Hiroshi Hasegawa[a], Masato Eto[b], Koichi Kozaki[a], Kenji Toba[a]

[a] *Department of Geriatric Medicine, Kyorin University School of Medicine, Tokyo, Japan*
[b] *Department of Geriatric Medicine, Graduate School of Medicine, University of Tokyo, 7-3-1 Hongo, Bunkyo-ku, Tokyo 113-8655, Japan*

Received 28 November 2005; received in revised form 9 May 2006; accepted 19 May 2006
Available online 27 June 2006

Abstract

Objective: Effects of potent free radical scavenger, edaravone, on oxidative stress-induced endothelial damage and early atherosclerosis were investigated using animal models and cultured cells.

Methods and results: Endothelial apoptosis was induced by 5-min intra-arterial exposure of a rat carotid artery with 0.01 mmol/L H_2O_2. Edaravone treatment (10 mg/kg i.p.) for 3 days suppressed endothelial apoptosis, as evaluated by chromatin staining of *en face* specimens at 24 h, by approximately 40%. Similarly, edaravone dose-dependently inhibited H_2O_2-induce apoptosis of cultured endothelial cells in parallel with the inhibition of 8-isoprostane formation, 4-hydroxy-2-nonenal (4-HNE) accumulation and VCAM-1 expression. Next, apolipoprotein-E knockout mice were fed a high-cholesterol diet for 4 weeks with edaravone (10 mg/kg i.p.) or vehicle treatment. Edaravone treatment decreased atherosclerotic lesions in the aortic sinus (0.18 ± 0.01 to 0.09 ± 0.01 mm^2, $P < 0.001$) and descending aorta (5.09 ± 0.86 to 1.75 ± 0.41 mm^2, $P < 0.05$), as evaluated by oil red O staining without influence on plasma lipid concentrations or blood pressure. Dihydroethidium labeling and cytochrome *c* reduction assay showed that superoxide anions in the aorta were suppressed by edaravone. Also, plasma 8-isoprostane concentrations and aortic nitrotyrosine, 4-HNE and VCAM-1 contents were decreased by edaravone treatment.

Conclusions: These results suggest that edaravone may be a useful therapeutic tool for early atherosclerosis, pending the clinical efficacy.

Keywords: Atherosclerosis; Reactive oxygen species; Free radical scavenger; Edaravone; 4-HNE; Apolipoprotein E knockout mouse

1. Introduction

Accumulating evidence has shown that stress-induced injury of vascular endothelial cells (ECs) is an initial event in the development of atherosclerosis [1]. In particular, oxidative stress has been implicated in endothelial injury caused by oxidized LDL and smoking as well as hypertension, diabetes and ischemia-reperfusion [1–3]. This notion is supported by the findings that the production of reactive oxygen species (ROS) is upregulated in vascular lesions [4,5], and that lesion formations such as endothelial dysfunction [6] and atherosclerosis [7] are accelerated by superoxide anion ($O_2^{\bullet -}$).

Experimental studies have shown the protective effects of antioxidants on atherosclerosis and endothelial injury. Dietary antioxidants were reported to preserve endothelial function [8,9] and inhibit atherosclerosis [10] in cholesterol-fed rabbits. In a well employed animal model of atherosclerosis, apolipoprotein E knockout (ApoE-KO) mouse fed a high fat diet, it has been shown that there was a significant increase in basal superoxide products [11,12], and that both $O_2^{\bullet -}$ levels and aortic lesion areas were attenuated by treatment with Vitamin E [11] or superoxide dismutase [13]. By contrast, it has been reported that elimination of NAD(P)H oxidase [14] or disruption of its subunit p47phox [15] had no effect on lesion size in ApoE-KO mice. Clinical experiments have

* Corresponding author. Tel.: +81 3 5800 8832; fax: +81 3 5800 8831.
E-mail address: akishita-tky@umin.ac.jp (M. Akishita).

0021-9150/$ – see front matter © 2006 Elsevier Ireland Ltd. All rights reserved.
doi:10.1016/j.atherosclerosis.2006.05.040

also shown that antioxidants such as Vitamins C and E can ameliorate endothelial dysfunction in patients with hypercholesterolemia or atherosclerosis [16,17], although recent clinical trials have failed to prove the protective effects of Vitamin E on cardiovascular events in patients with risk factors [18] and in healthy subjects [19].

Edaravone is a potent free radical scavenger that has been clinically used to reduce the neuronal damage following ischemic stroke [20]. Edaravone has promising property to quench hydroxyl radical ($^{\bullet}OH$) and show inhibitory effects on peroxynitrite ($ONOO^-$) and both water-soluble and lipid-soluble peroxyl radical ($LOO^{\bullet}$) [21,22]. Accordingly, this compound exerts a wide range of antioxidant activity on ROS beyond the effects of water-soluble or lipid-soluble antioxidant vitamins. Based on this idea, we hypothesized that edaravone would inhibit the process of atherosclerosis.

To test this hypothesis, we investigated the effects of edaravone in two experimental models. First, we examined whether edaravone could inhibit hydrogen peroxide (H_2O_2)-induced EC apoptosis in a rat model [23] and cultured ECs. Second, we examined whether edaravone could suppress the atherosclerotic lesion formation in ApoE-KO mice.

2. Methods

2.1. Animals

Male Wistar rats aged 10–12 weeks (Japan Clea), and male C57BL/6 mice and ApoE-KO mice on C57BL/6 background aged 4–6 weeks (Jackson Laboratory) were used in this study. All of the experimental protocols were approved by the Animal Research Committee of the Kyorin University School of Medicine.

2.2. H_2O_2-induced EC apoptosis in rats and in culture

EC apoptosis was induced by 5-min intra-arterial treatment of a rat carotid artery with 0.01 mmol/L H_2O_2 as previously described [23]. Briefly, edaravone (3-methyl-1-phenyl-2-pyrazolin-5-one; 3 or 10 mg/kg; donated by Mitsubishi Pharma Corporation, Japan) or its vehicle was intraperitoneally injected daily for 3 days before H_2O_2 treatment. A catheter was placed in the common carotid artery via the external carotid artery. The lumen was flushed with saline, replaced with 0.01 mmol/L H_2O_2 diluted with saline for 5 min and recovered. At 24 h after H_2O_2 treatment, EC apoptosis was evaluated by chromatin staining of *en face* specimens of the carotid artery using Hoechst 33342 dye. Apoptotic cells were identified by their typical morphological appearance; chromatin condensation, nuclear fragmentation, or apoptotic bodies. The numbers of apoptotic cells and intact cells were counted in 10 high-power fields for each specimen by an observer blinded to the treatment group.

Apoptosis of ECs isolated from a bovine carotid artery was induced as previously described [24]. Briefly, subconfluent ECs were pretreated for 24 h with culture medium containing edaravone or vehicle. After washing twice with Hank's balanced salt solution, the cells were exposed to H_2O_2 (0.2 mmol/L) diluted in Hank's balanced salt solution for 1.5 h at 37 °C to induce apoptosis. Then ECs were cultured in culture medium containing edaravone or vehicle until assay. Apoptosis was evaluated at 24 h after H_2O_2 treatment as histone-associated DNA fragments using a photometric enzyme immunoassay (Cell Death Detection ELISA, Roche), according to the manufacturer's instructions.

2.3. Atherosclerosis in ApoE-KO mice

ApoE-KO mice received a high-cholesterol diet (1% cholesterol, 10% fat in CE-2 standard diet; Japan Clea) for 4 weeks. Simultaneously, edaravone (10 mg/kg) or its vehicle was intra-peritoneally injected daily throughout the experiments. Body weight and systolic blood pressure were recorded every week in a conscious state by the tail cuff method (BP-98A; Softron, Tokyo).

At 4 weeks of treatment, mice were sacrificed with an overdose of diethyl ether and perfusion-fixed. Atherosclerotic lesions in the aortic sinus were quantified according to the method described previously [25]. We also measured the surface area of atherosclerotic lesions in the whole descending aorta including the abdominal aorta just proximal to the iliac bifurcation. *En face* specimens of the descending aorta were stained with oil red O, photographed and analyzed using the NIH image software. Total cholesterol, high-density lipoprotein cholesterol and low-density lipoprotein cholesterol in mice plasma were determined by a commercial laboratory (SRL, Japan).

2.4. Measurement of ROS

Aortic samples for ROS measurements were prepared separately from those for atherosclerosis evaluation. At 4 weeks of treatment, ApoE-KO mice were sacrificed with CO_2 inhalation. Descending aortas were rapidly removed and placed into chilled modified Krebs/HEPES buffer. C57BL/6 mice fed a standard diet were also used as the control. To determine superoxide production *in situ*, frozen cross-sections of the aorta were stained with 10 μmol/L dihydroethidium (DHE; Molecular Probes), followed by fluorescent microscopy [26]. Also, superoxide production in aortic rings was quantified using the superoxide dismutase-inhibitable cytochrome *c* reduction assay as previously described [27]. Immunohistochemical detection of 3-nitrotyrosine in the aorta was visualized by diaminobenzidine as reported previously [28].

Intracellular production of superoxide anions was measured using DHE as described previously [29], and the intensity values were calculated using the Metamorph software [24]. Concentrations of 8-isoprostane (8-iso prostaglandin

$F_{2\alpha}$) in the culture supernatants and mouse plasma were measured using a commercially available EIA kit (Cayman Chemical). Culture supernatants were directly applied to EIA, while plasma was applied to EIA after solid phase extraction purification according to the manufacturer's instructions.

2.5. Western blotting

Western blotting was performed as previously described [30], to detect the expression of VCAM-1 and 4-HNE in cultured ECs and mouse aortas. Descending aortas were prepared as described in ROS measurements. The antibodies used in this study were anti-4-HNE monoclonal antibody (JaICA, Shizuoka, Japan), anti-VCAM-1 polyclonal antibody (Santa Cruz Biotechnology) and anti-3-nitrotyrosine monoclonal antibody (Upstate). Densitometric analysis was performed using an image scanner and the NIH software.

2.6. Data analysis

All values are express as mean ± S.E.M. Data were analyzed using one-factor ANOVA. If a statistically significant effect was found, Newman–Keuls' test was performed to isolate the difference between the groups. Differences with a value of $P < 0.05$ were considered statistically significant.

3. Results

3.1. Effects of edaravone on H_2O_2-induced EC apoptosis and ROS

As shown in Fig. 1A, edaravone dose-dependently inhibited EC apoptosis in culture, which was induced 24 h after H_2O_2 treatment. Edaravone was then employed in a rat model of H_2O_2-induced EC apoptosis. Consistent with the *in vitro* experiment, edaravone of 10 mg/kg/day decreased EC apoptosis of the rat carotid artery by approximately 40% (Fig. 1B).

We next examined whether edaravone decreased ROS production in the process of H_2O_2-induced EC apoptosis. For this purpose, DHE fluorescent, a marker of intracellular production of superoxide anions, release of 8-isoprostane into the culture supernatants and accumulation of 4-HNE, a pivotal end-product of lipid peroxidation [31], were measured using cultured ECs. We also examined the expression of VCAM-1 as a marker of endothelial injury or activation [32]. Edaravone decreased DHE fluorescent, 8-isoprostane formation and VCAM-1 expression at 3 h after H_2O_2 treatment in a dose-dependent manner (Fig. 2A–C). As shown in Fig. 2D, multiple bands showing 4-HNE-Michael protein adducts [33,34] were accumulated after H_2O_2 treatment in a time-dependent manner. Consequently, the effect of edaravone on 4-HNE expression was examined at 3 h after H_2O_2 treatment (4.5 h after H_2O_2 was initially added). Edaravone decreased 4-HNE expression in a dose dependent manner.

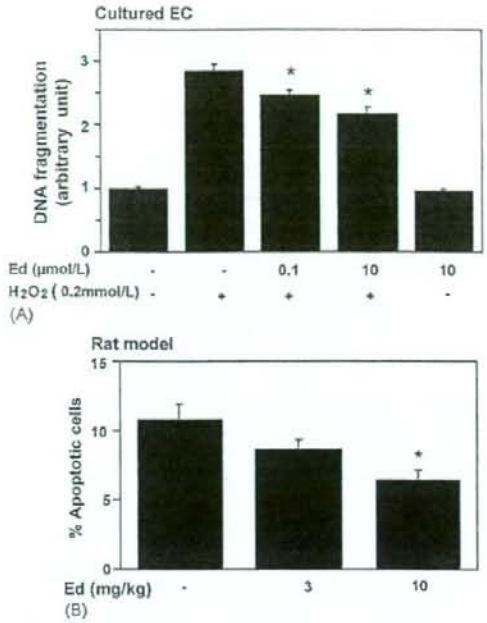

Fig. 1. Effects of edaravone (Ed) on H_2O_2-induced EC apoptosis in culture (A) and in a rat model (B). (A) Ed or its vehicle was added to the culture medium 24 h before H_2O_2 treatment until assay. EC apoptosis was evaluated 24 h after H_2O_2 treatment (0.2 mmol/L) by means of DNA fragmentation. Values are expressed as mean ± S.E.M. ($n = 3$). $^*P < 0.05$ vs. H_2O_2 (+) + Ed (−). (B) Ed or its vehicle was intraperitoneally injected once a day for 3 days before H_2O_2 treatment. At 24 h after H_2O_2 treatment, apoptotic ECs were counted per high power field and the ratio of the apoptotic cell number to the intact cells was calculated using *en face* specimens of the carotid artery stained with Hoechst 33342. Values are expressed as mean ± S.E.M. ($n = 7$). $^*P < 0.05$ vs. vehicle.

3.2. Effects of edaravone on atherosclerotic lesions and ROS in ApoE-KO mice

In the next set of experiments, we examined whether edaravone could suppress the atherosclerotic lesions in ApoE-KO mice fed a high cholesterol diet for 4 weeks. As shown in Fig. 3A and B, atheromatous lesions both in the aortic sinus and the descending aorta were smaller in mice treated with 10 mg/kg/day edaravone than in those with vehicle. This dose of edaravone did not influence body weight, blood pressure or plasma LDL and HDL cholesterol levels (Table 1).

Then, we examined whether the anti-atherogenic effects of edaravone were associated with the decrease in ROS production. Peroxynitrite formation was assessed as 3-nitrotyrosine accumulation in the aorta [28]. Both immunohistochemistry and Western blotting showed that edaravone inhibited nitrotyrosine accumulation in the aorta of ApoE-KO mice (Fig. 4A(a) and A(b)). Superoxide production *in situ* was examined using DHE staining of the descend-

Table 1
Body weight, blood pressure and plasma lipid levels in ApoE-KO mice treated with edaravone or vehicle

	Vehicle	Edaravone
Body weight (g)	21.4 ± 0.5	21.0 ± 0.5
Systolic blood pressure (mmHg)	106 ± 2	103 ± 3
Total cholesterol (mg/dL)	1967 ± 38	1872 ± 66
HDL cholesterol (mg/dL)	66 ± 6	82 ± 9
LDL cholesterol (mg/dL)	602 ± 24	602 ± 12

The values are shown as mean ± S.E. ($n = 14$). There were no significant differences in the values between the two groups.

ing aorta. As shown in Fig. 4B, ethidium fluorescence, which was amplified in ApoE-KO mice, was decreased by edaravone treatment. A quantitative analysis by the superoxide dismutase-inhibitable cytochrome *c* reduction assay revealed that $O_2^{\bullet -}$ levels in aortic rings of ApoE-KO mice were decreased by 43% in edaravone-treated ApoE-KO mice compared to those in vehicle-treated mice (Fig. 4C). Consistent with these results, plasma 8-isoprostane levels and 4-HNE expression in the descending aorta, both of which were elevated in ApoE-KO mice compared to

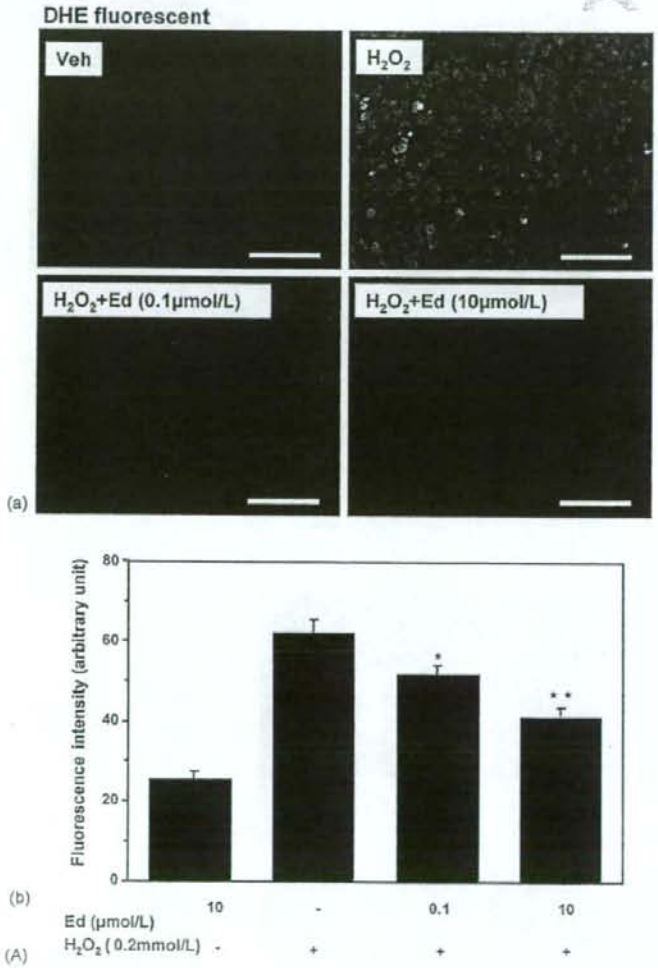

Fig. 2. Effects of edaravone (Ed) on DHE fluorescent (A) and 8-isoprostane formation (B), VCAM-1 expression (C) and 4-HNE expression (D) in cultured EC. Ed or its vehicle was added to the culture medium 24 h before H_2O_2 treatment until assay. DHE fluorescent ($n = 6$), 8-isoprostane concentration ($n = 3$) and VCAM-1 expression ($n = 3$) in the cell lysate were measured 3 h after H_2O_2 treatment. Values are expressed as mean ± S.E.M. Time dependent changes of 4-HNE expression after H_2O_2 treatment was detected by Western blotting. Representative image showed that 4-HNE-Michael protein adducts were accumulated after treatment (D(a)). The major 97 kDa band was measured 4.5 h after H_2O_2 treatment in the presence or absence of edaravone (D(b)). Values are expressed as mean ± S.E.M. ($n = 3$). $^{*}P < 0.05$, $^{**}P < 0.01$ vs. H_2O_2 (+) + Ed (−).

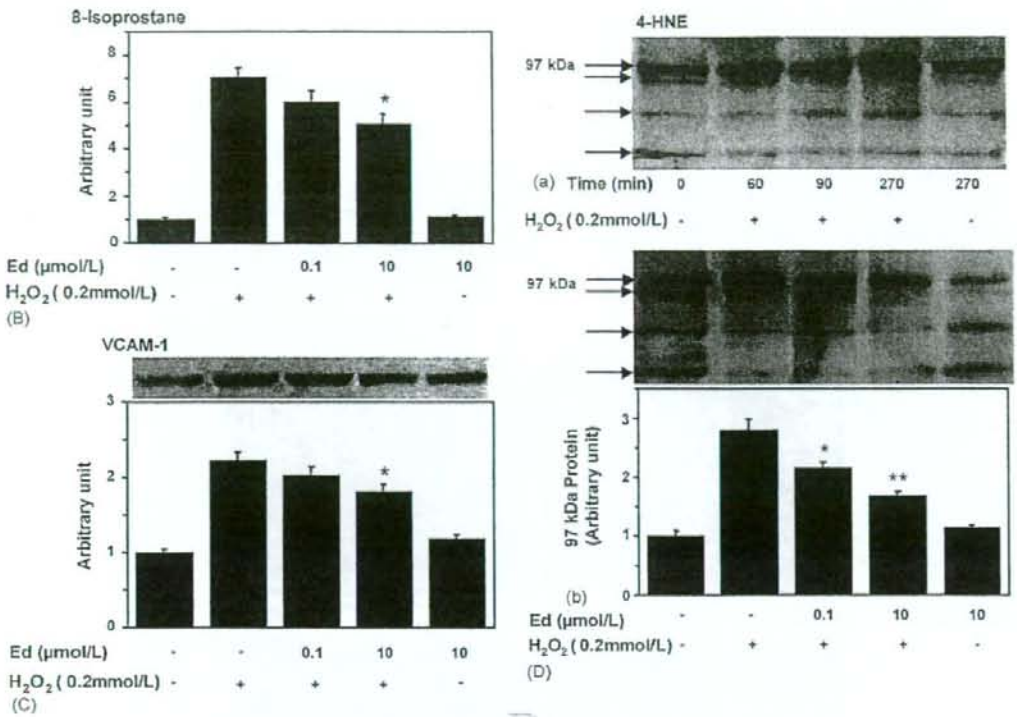

Fig. 2. (*Continued*).

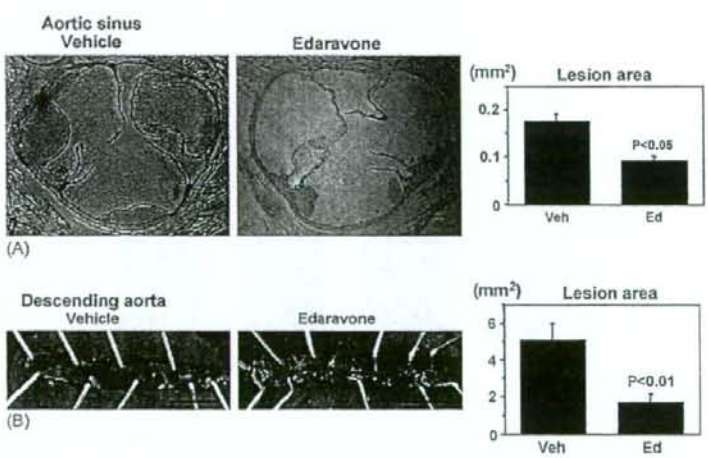

Fig. 3. Effects of edaravone on atherosclerotic lesion in ApoE-KO mice. ApoE-KO mice were fed a high-cholesterol diet for 4 weeks with the administration of edaravone (10 mg/kg daily) or its vehicle by i.p. injection. (A) Oil red O-stained cross-sections of the aortic sinus (bar = 100 μm) and morphometric analysis of the lesions are shown. (B) Oil red O-stained *en face* specimens of the descending aorta (bar = 5 mm) and morphometric analysis of the lesions are shown. Values are expressed as mean ± S.E.M. ($n = 14$).

those in wild-type C57BL/6 mice fed a normal chow, were decreased by edaravone treatment (Fig. 4D and E). Finally, the increase in VCAM-1 expression in the aorta of ApoE-KO mice was attenuated by edaravone as well (Fig. 4F).

4. Discussion

A number of studies have shown that ROS contribute to the pathogenesis of endothelial dysfunction and atherosclerosis formation. In addition to $O_2^{\bullet -}$ that is predominantly pro-

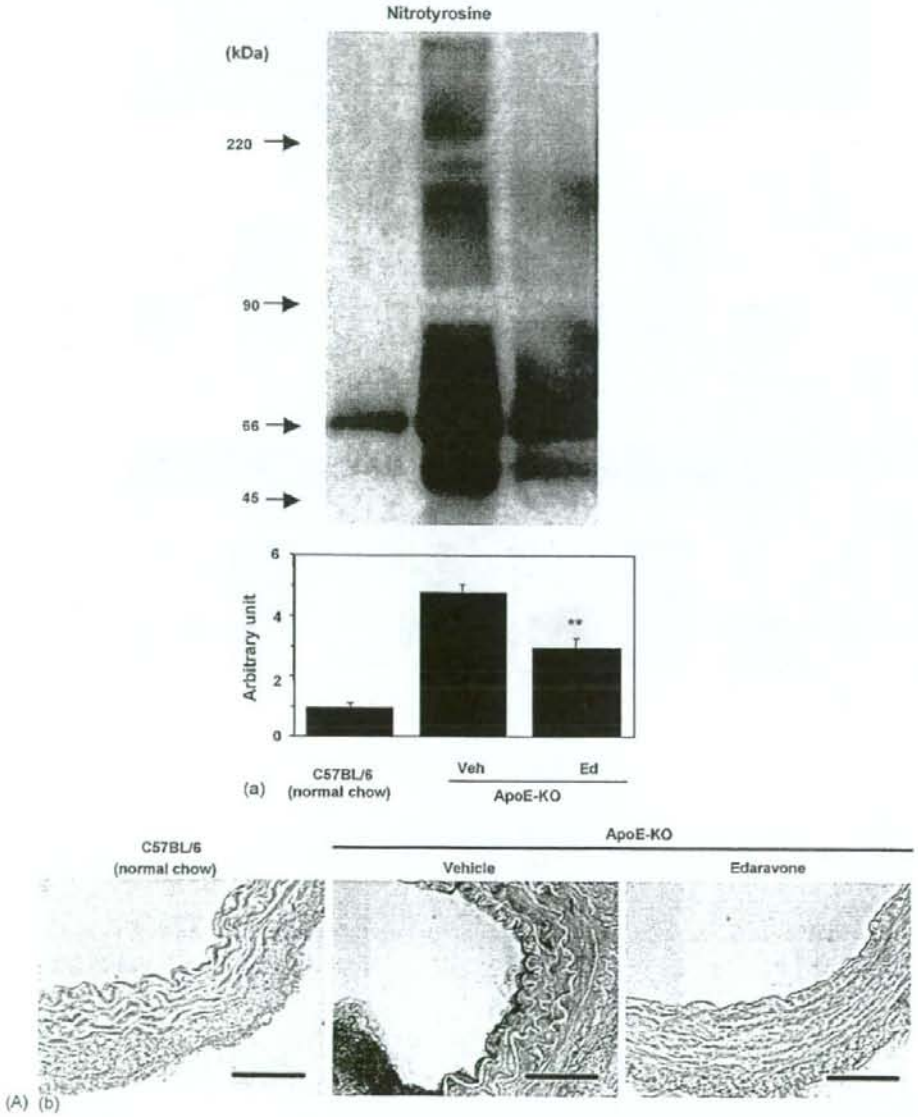

Fig. 4. Effects of edaravone (Ed) on ROS production (A–E) and VCAM-1 expression (F) in ApoE-KO mice. (A) Nitrotyrosine contents in the aorta was examined by Western blot analysis (A(a), $n=6$) and immunohistochemistry (A(b)). Bar = 50 μm. (B) Fresh-frozen cross-sections of the aorta were stained with DHE, and representative fluorescent micrographs are shown (bar = 100 μm). (C) Superoxide anion in aortic rings was determined using SOD inhibitable-cytochrome *c* reduction assay ($n=6$). (D) 8-Isoprostane level in mouse plasma was measured with EIA ($n=6$). (E and F) Representative Western blotting for 4-HNE (97 kDa band) and VCAM-1 expression in the aorta and densitometric analysis are shown ($n=3$). Values are expressed as mean ± S.E.M. $^{*}P<0.05$, $^{**}P<0.01$ vs. vehicle (Veh). C57/BL6 mice fed a normal chow serve as the control.